CHEMISTRY OF MATERIALS
Cite This: Chem. Mater. 2017, 29, 10284−10288
Communication
pubs.acs.org/cm

Infinite Coordination Polymer Particles Composed of Stimuli-Responsive Coordination Complex Subunits

Andrea I. d'Aquino, Zachary S. Kean, and Chad A. Mirkin*

Department of Chemistry and International Institute for Nanotechnology, Northwestern University, 2145 Sheridan Road, Evanston, Illinois 60208, United States

Supporting Information

Infinite coordination polymer particles (ICPs) are organic−inorganic hybrid materials in which repeating ligand units are connected via metal ion nodes into one-, two-, or three-dimensional structures.[1] Interest in ICPs stems from their modularity, ease in which organic components can be interchanged within them, and how changes in molecular structure can result in changes in porosities,[2] as well as catalytic,[3] biological,[4] and spectroscopic properties.[5] While this broad class of materials encompasses polymers with regular repeat units, such as crystalline metal−organic frameworks (MOFs) and other nano- or porous coordination polymers (NCPs or PCPs), the scope of ICPs is not limited to crystalline materials. Work by our group[6−8] and others[9−11] has shown that amorphous ICPs can be formed under the kinetically controlled precipitation of soluble precursors. The ability to assume an amorphous state enables the formation of nano- and micrometer-sized particles where shape is not dictated by crystal packing forces but instead by the interfacial free energy between the particles and the solvent.[12] Initial work from our group and others[7,9] reported the first methods for synthesizing spherical ICP particles. Since this initial work, the library of building blocks and ICP particles accessible through this approach has grown significantly,[7,13−15] and, importantly, these studies have demonstrated that the chemical and physical properties of these materials are highly morphology-dependent.

An attractive feature of ICP particles is their ability to incorporate a wide variety of complex building blocks, including ones that render such structures stimuli-responsive.[16] One class of architectures yet to be explored in the context of ICP particles are ones made from Weak-Link Approach (WLA) building blocks. WLA complexes are supramolecular coordination compounds that are assembled from transition metal precursors (typically d^8 metal centers) and hemilabile ligands. They are defined by both open (flexible) and closed (rigid) structural states that may be interconverted through the introduction or removal of chemical effectors (Scheme 1A,B).[17] They have shown promise in amplified chemical sensing,[18−20] catalysis,[21] and molecular recognition.[22] Although they have not yet been studied in polymeric systems and ICPs in particular, they could prove to be valuable modalities for modulating both the chemical and the physical properties of such structures in a postsynthetic manner, as they provide precise chemical control over molecular geometry, charge, and flexibility of the molecular subunits and resulting oligomers. Herein, we report the design and synthesis of a new class of ICP particles consisting of ferric ions and chemically addressable WLA complex building blocks. These structures have been characterized in the presence and absence of an elemental ion effector (Cl^-), which changes the local coordination environment of the metal nodes within the polymer, in addition to the mesoscopic structural fate of the particle.

Scheme 1. WLA Complexes Containing Hemilabile Coordinating Motifs Can Be Toggled between Open (flexible) (A) and Closed (rigid) States (B)[a] and Coordination-Based Assembly of These Subunits Results in Extended Structures (C, D)

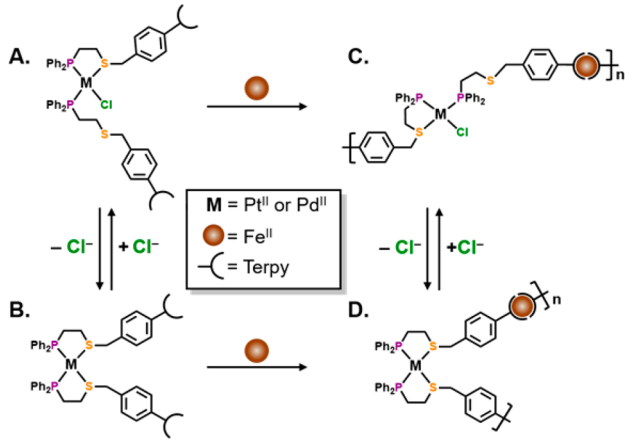

[a]Counterions omitted for clarity.

Proof-of-concept WLA-based ICPs were synthesized from monomers composed of (1) either square-planar Pt^{II} or Pd^{II} metal cores bound to hemilabile phosphino−thioether (P,S) ligands appended with (2) a secondary terpyridine ligand. The terpyridine moieties allow such complexes to be oligomerized and polymerized in the presence of Fe^{II} ions (Scheme 1C,D).

We first synthesized ligand **1** (Figure 1A) according to a modified literature procedure from previously reported compounds (see Supporting Information).[23] We chose the terpyridine moiety for its extremely high affinity ($K_a \sim 10^8$) and selective 2:1 binding with Fe^{II} ions,[24] as well as the previously demonstrated orthogonality of this binding motif with Pt^{II}−WLA systems.[23] Ligand **1** was then reacted with dichloro(1,5-cyclooctadiene) platinum(II) ($Pt(COD)Cl_2$) in dichlorome-

Received: August 28, 2017
Revised: December 8, 2017
Published: December 14, 2017

DOI: 10.1021/acs.chemmater.7b03638
Chem. Mater. 2017, 29, 10284−10288

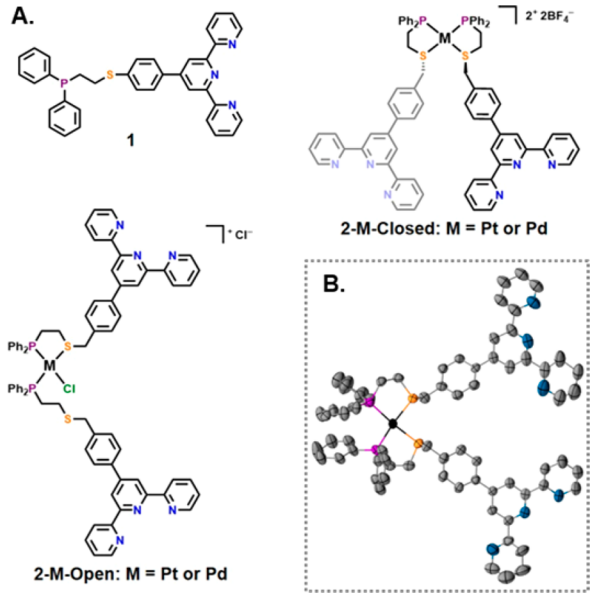

Figure 1. (A) Molecular building blocks used in the synthesis of ICP particles bearing WLA subunits. (B) X-ray crystal structure of complex **2-Pt-Closed**, drawn with 50% thermal ellipsoid probability. Hydrogens, solvent molecules, and anions have been omitted for clarity (black, platinum; orange, sulfur; purple, phosphorus; gray, carbon; blue, nitrogen).

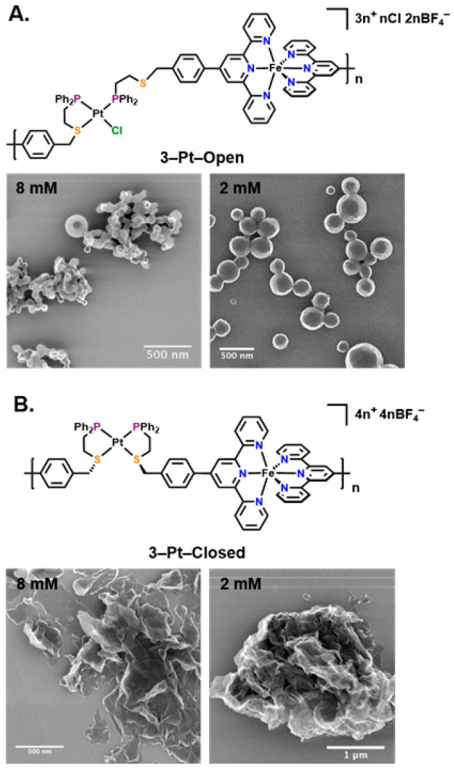

Figure 2. Proposed repeat unit, coordination polymer structure (top), and STEM micrographs (bottom) of ICPs bearing (A) open and (B) closed WLA subunits at different concentrations.

thane (CH_2Cl_2) to yield complex **2-Pt-Open** (Figure 1A) in quantitative yield.

The molecular structure of **2-Pt-Open** is both flexible and dynamic, whereby exchange between the thioether group and the chloride (Cl^-) bound to the Pt^{II} center occurs at room temperature as evidenced by variable temperature ^{31}P nuclear magnetic resonance (NMR) spectroscopy (see Supporting Information). With complex **2-Pt-Open** in hand, we were able to generate the rigid complex **2-Pt-Closed** (Figure 1A) by chloride abstraction with thallium tetrafluoroborate ($TlBF_4$). The structure and geometry of complex **2-Pt-Closed** were confirmed in solution by ^1H and ^{31}P NMR spectroscopies and high-resolution electrospray ionization mass spectrometry (HR-ESI-MS) and in the solid-state by single crystal X-ray diffraction (Figure 1B).

To form soluble ICP precursors, both **2-Pt-Open** and **2-Pt-Closed** were dissolved in acetonitrile (CH_3CN) and treated with one equivalent of iron(II) tetrafluoroborate ($Fe(BF_4)_2$) to polymerize the terpyridine groups to form the intermediates **3-Pt-Open** and **3-Pt-Closed**, respectively (Figure 2), which can be switched between states post polymerization (see Supporting Information). While the ^1H NMR spectrum of **3-Pt-Open** was relatively nondescript, comprised of many broad peaks and consistent with the formation of high molecular weight polymer, the ^1H NMR spectrum of **3-Pt-Closed** exhibited well-formed narrow peaks and was more complex, consistent with more rigid and less dynamic species (see Supporting Information, Figures S2 and S3).

To further characterize these structures, diffusion-ordered spectroscopy (DOSY) experiments were performed. Based on the ^1H DOSY experiments, the diffusion coefficient of **3-Pt-Closed** is calculated to be approximately a factor of four greater than the constituent monomer **2-Pt-Closed**, as calculated from the Stokes–Einstein equation (see Supporting Information, Figures S4 and S5), indicating the formation of low molecular weight, cyclic oligomers. This result is consistent with the narrow peaks present in the ^1H NMR spectrum of **3-Pt-Closed** and can be attributed to the nearly coparallel orientation of the terminal terpyridine ligands. This observation is consistent with that of analogous systems[25−28] and with density functional theory (DFT) calculations performed on the solid-state structure of **3-Pt-Closed** (see Supporting Information, Figure S6). It is clear that the flexible nature of the monomer **2-Pt-Open** enables the formation of flexible coordination polymer **3-Pt-Open** in solution. The closed monomer (**2-Pt-Closed**), however, results in the formation of rigid cyclic oligomers (**3-Pt-Closed**) owing to the coparallel orientation of the terminal terpyridines ligands. This coparallel orientation is a direct result of the nearly 30° angle formed between the Pt^{II} metal node and the thioether moiety on the P,S-ligand, in the closed structure. The results observed for the soluble precursors indicate that molecular geometry strongly affects the nature of the polymeric precursors and, ultimately, particle morphology.

Next, we synthesized ICP particles by the slow precipitation method.[7,29] In a typical experiment, a solution of either **3-Pt-Open** or **3-Pt-Closed** was prepared in CH_3CN, and diethyl ether was allowed to slowly diffuse into it over the course of 24 h. Particle samples were then suspended in an excess of diethyl ether for storage and analysis. All samples were analyzed by scanning transmission electron microscopy (STEM) and energy-dispersive X-ray spectroscopy (EDX), indicating an elemental composition consistent with the proposed structures (see Supporting Information), while samples that formed stable suspensions were also characterized by dynamic light scattering (DLS) (see Supporting Information, Figure S13). Importantly, the morphology of the final particles formed from **3-Pt-Open** was highly dependent on the concentration of the initial

DOI: 10.1021/acs.chemmater.7b03638
Chem. Mater. 2017, 29, 10284−10288

solution in acetonitrile. When particles were grown from an 8 mM solution (with respect to the monomer) of **3-Pt-Open**, the resulting particles were composed of spherical aggregates and particles of various sizes, with most spherical features being smaller than 100 nm; this is consistent with uncontrolled growth and incomplete coalescence characteristic of conditions where growth occurs too quickly (Figure 2A).[7]

Alternatively, when the concentration was lowered to 2 mM, we obtained spherical particles between 200 and 500 nm in size (DLS Z-Average size = 195 nm, see Figure S9) that, while well formed, appeared to have rough surface features. While **3-Pt-Open** under 8 mM growth conditions was observed to form particles with predominantly spherical features, the oligomeric precursor **3-Pt-Closed** yielded ill-defined aggregates and sheets. Synthesis of particles was also attempted with substoichiometric quantities of chloride, and two kinds of morphologies were observed: aggregates of spherical particles and sheets (see Supporting Information). When the concentration of the **3-Pt-Closed** was lowered to 2 mM, larger aggregates were formed (Figure 2B). While we attempted to further slow the growth process by performing the particle synthesis at ∼5 °C, this simply arrested the growth process at stages that resulted in ill-defined aggregates of small spheres (see Supporting Information).

In light of our inability to grow smooth, well-defined ICP particles, we looked toward adjusting the strength of the metal−ligand coordination bonds as a means of facilitating molecular level rearrangement and more rapid coalescence of the system. Here, we hypothesized that by employing a more labile metal center, smooth spheres would form in order to minimize interfacial energy, as any rough surface topology will increase the overall surface area and thus the interfacial energy. To test this hypothesis, we took advantage of the modular nature of the WLA to assemble a new set of complexes with an isoelectronic and isostructural palladium core. Previous reports indicate that the rate of Pd−P,S-ligand exchange occurs on the time scale of seconds and minutes,[30] much faster than that for Pt−P,S-ligand exchange under identical conditions. Therefore, we utilized modified procedures to synthesize a new set of monomers, **2-Pd-Open** (Figure 3A) and **2-Pd-Closed**, which are qualitatively identical to the Pt derivatives, as evidenced by ^{1}H NMR spectroscopy, ^{1}H DOSY, ESI mass spectrometry, and single crystal X-ray diffraction studies (see Supporting Information). Importantly, coordination polymers **3-Pd-Open** and **3-Pd-Closed** can be synthesized and interconverted post polymerization, which was confirmed by ^{1}H and ^{31}P NMR spectroscopy and DOSY experiments (see Supporting Information).

ICP formation was attempted again by slow diffusion of diethyl ether into acetonitrile solutions of **3-Pd-Open** or **3-Pd-Closed** (2 and 8 mM). Intriguingly, while there were some variations in size and polydispersity, all samples led to the formation of well-formed spherical particles with smooth surface topologies (Figure 3). The variation in size between **3-Pd-Open** and **3-Pd-Closed** is likely due to the difference in length between the monomers that comprise the two polymeric states. The open states, regardless of metal, are extended and more flexible than the closed states.

This observation not only supports our hypothesis that the formation of smooth spheres will result from employing a more labile metal center but also rules out the potential effect of charge and counterions on the particle morphology. For example, between the open and the closed systems the charge

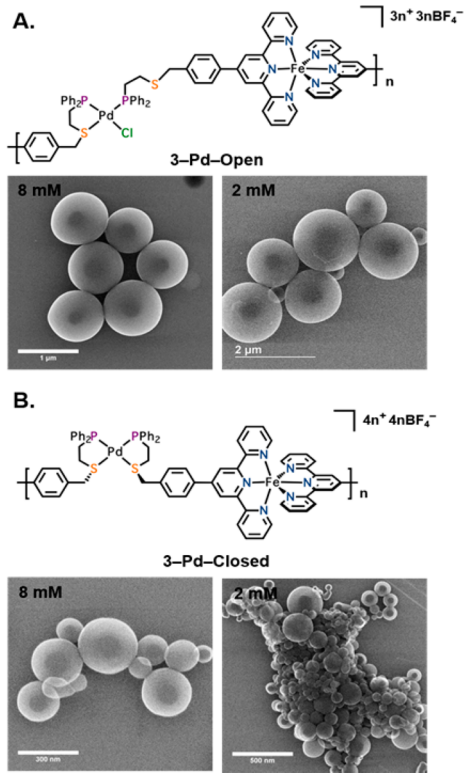

Figure 3. Proposed repeat unit structure (top) and STEM micrographs (bottom) of ICPs bearing (A) open and (B) closed palladium WLA subunits.

changes from 1^{+} to 2^{+}, as do the counterions (Cl^{-} to BF_4^{-}); however, this in itself has no bearing on the final morphology given that both **3-Pd-Open** or **3-Pd-Closed** form particles of the same morphology. During the slow diffusion of the initiation solvent (diethyl ether), the concentrations of the ligand and metal ion precursors decrease over time, resulting in a decrease in the nucleation of new particles.[1] Although physical parameters, such as concentration and temperature, were used to control the rate at which nucleation and particle formation occur, achieving monodisperse particles remains a challenge for these amorphous materials.

In conclusion, when taken together, these results indicate that the ability of the system to rearrange on the molecular level dictates its ability to form fully coalesced smooth ICP particles. This study also suggests that one can use switchable molecular motifs embedded within ICPs to control morphology and that metal-heteroatom bond strength (Pt−P,S vs Pd−P,S) is an important consideration and point of tunability. Indeed, if the interactions are too weak, as in the case of the Pd system, very little differentiation at the mesoscopic particle level is observed under all conditions tested. These observations open the door to making well-defined ICP particles with stimuli-responsive units embedded within and for controlling particle morphology by altering the lability of coordination bonds in particles formed under kinetic control. Such structures may lead to new motifs that could become important in the area of chemical sensing where molecularly triggered events can lead to changes in macroscopic properties that affect signaling.

DOI: 10.1021/acs.chemmater.7b03638
Chem. Mater. 2017, 29, 10284−10288

■ ASSOCIATED CONTENT

Supporting Information

The Supporting Information is available free of charge on the ACS Publications website at DOI: 10.1021/acs.chemmater.7b03638.

Experimental details, including 2D DOSY spectra, DLS data, STEM and EDX data, and NMR spectra (PDF)
Crystallographic data (CIF)
Crystallographic data (CIF)

■ AUTHOR INFORMATION

Corresponding Author

*(C.A.M.) E-mail: chadnano@northwestern.edu.

ORCID

Chad A. Mirkin: 0000-0002-6634-7627

Author Contributions

C.A.M. directed the research. A.I.D. and Z.S.K. carried out the experiments, and the manuscript was written through contributions from all of the authors. All authors have given approval to the final version of the manuscript.

Notes

The authors declare no competing financial interest.

■ ACKNOWLEDGMENTS

This material is based upon work supported by the U.S. Army Grant W911NF-15-1-0151 and the National Science Foundation Grants CHE-1149314 and CHE-1709888. A.I.D. acknowledges a National Science Foundation Graduate Research Fellowship, and Z.S.K. acknowledges an International Institute for Nanotechnology (IIN) Postdoctoral Fellowship.

■ REFERENCES

(1) Spokoyny, A. M.; Kim, D.; Sumrein, A.; Mirkin, C. A. Infinite coordination polymer nano- and microparticle structures. *Chem. Soc. Rev.* **2009**, *38*, 1218−1227.

(2) Ferey, G. Hybrid porous solids: past, present, future. *Chem. Soc. Rev.* **2008**, *37*, 191−214.

(3) Park, K. H.; Jang, K.; Son, S. U.; Sweigart, D. A. Self-supported organometallic rhodium quinonoid nanocatalysts for stereoselective polymerization of phenylacetylene. *J. Am. Chem. Soc.* **2006**, *128*, 8740−8741.

(4) Calabrese, C. M.; Merkel, T. J.; Briley, W. E.; Randeria, P. S.; Narayan, S. P.; Rouge, J. L.; Walker, D. A.; Scott, A. W.; Mirkin, C. A. Biocompatible Infinite-Coordination-Polymer Nanoparticle−Nucleic-Acid Conjugates for Antisense Gene Regulation. *Angew. Chem., Int. Ed.* **2015**, *54*, 476−480.

(5) Jeon, Y. M.; Heo, J.; Mirkin, C. A. Dynamic interconversion of amorphous microparticles and crystalline rods in salen-based homochiral infinite coordination polymers. *J. Am. Chem. Soc.* **2007**, *129*, 7480−7481.

(6) Oh, M.; Mirkin, C. A. Ion exchange as a way of controlling the chemical compositions of nano- and microparticles made from infinite coordination polymers. *Angew. Chem., Int. Ed.* **2006**, *45*, 5492−5494.

(7) Oh, M.; Mirkin, C. A. Chemically tailorable colloidal particles from infinite coordination polymers. *Nature* **2005**, *438*, 651−654.

(8) Jeon, Y. M.; Armatas, G. S.; Kim, D.; Kanatzidis, M. G.; Mirkin, C. A. Troger's-Base-Derived Infinite Co-ordination Polymer Microparticles. *Small* **2009**, *5*, 46−50.

(9) Sun, X. P.; Dong, S. J.; Wang, E. K. Coordination-induced formation of submicrometer-scale, monodisperse, spherical colloids of organic-inorganic hybrid materials at room temperature. *J. Am. Chem. Soc.* **2005**, *127*, 13102−13103.

(10) Imaz, I.; Maspoch, D.; Rodríguez-Blanco, C.; Pérez-Falcón, J. M.; Campo, J.; Ruiz-Molina, D. Valence-Tautomeric Metal−Organic Nanoparticles. *Angew. Chem., Int. Ed.* **2008**, *47*, 1857−1860.

(11) Johnson, C. A.; Sharma, S.; Subramaniam, B.; Borovik, A. S. Nanoparticulate Metal Complexes Prepared with Compressed Carbon Dioxide: Correlation of Particle Morphology with Precursor Structure. *J. Am. Chem. Soc.* **2005**, *127*, 9698−9699.

(12) Spokoyny, A. M.; Kim, D.; Sumrein, A.; Mirkin, C. A. Infinite coordination polymer nano- and microparticle structures. *Chem. Soc. Rev.* **2009**, *38*, 1218−1227.

(13) Cho, W.; Lee, H. J.; Oh, M. Growth-Controlled Formation of Porous Coordination Polymer Particles. *J. Am. Chem. Soc.* **2008**, *130*, 16943−16946.

(14) Jung, S.; Oh, M. Monitoring shape transformation from nanowires to nanocubes and size-controlled formation of coordination polymer particles. *Angew. Chem., Int. Ed.* **2008**, *47*, 2049−2051.

(15) Farha, O. K.; Spokoyny, A. M.; Mulfort, K. L.; Galli, S.; Hupp, J. T.; Mirkin, C. A. Gas-Sorption Properties of Cobalt(II)-Carborane-Based Coordination Polymers as a Function of Morphology. *Small* **2009**, *5*, 1727−1731.

(16) Zhang, Y.; Guo, Y. J.; Wu, S. Y.; Liang, H. J.; Xu, H. X. Photodegradable Coordination Polymer Particles for Light-Controlled Cargo Release. *Acs Omega* **2017**, *2*, 2536−2543.

(17) Lifschitz, A. M.; Rosen, M. S.; McGuirk, C. M.; Mirkin, C. A. Allosteric Supramolecular Coordination Constructs. *J. Am. Chem. Soc.* **2015**, *137*, 7252−7261.

(18) Gianneschi, N. C.; Nguyen, S. T.; Mirkin, C. A. Signal Amplification and Detection via a Supramolecular Allosteric Catalyst. *J. Am. Chem. Soc.* **2005**, *127*, 1644−1645.

(19) Masar, M. S., III; Gianneschi, N. C.; Oliveri, C. G.; Stern, C. L.; Nguyen, S. T.; Mirkin, C. A. Allosterically Regulated Supramolecular Catalysis of Acyl Transfer Reactions for Signal Amplification and Detection of Small Molecules. *J. Am. Chem. Soc.* **2007**, *129*, 10149−10158.

(20) Yoon, H. J.; Mirkin, C. A. PCR-like cascade reactions in the context of an allosteric enzyme mimic. *J. Am. Chem. Soc.* **2008**, *130*, 11590−11591.

(21) Yoon, H. J.; Kuwabara, J.; Kim, J.-H.; Mirkin, C. A. Allosteric Supramolecular Triple-Layer Catalysts. *Science* **2010**, *330*, 66−69.

(22) Mendez-Arroyo, J.; Barroso-Flores, J.; Lifschitz, A. M.; Sarjeant, A. A.; Stern, C. L.; Mirkin, C. A. A Multi-State, Allosterically-Regulated Molecular Receptor With Switchable Selectivity. *J. Am. Chem. Soc.* **2014**, *136*, 10340−10348.

(23) Machan, C. W.; Adelhardt, M.; Sarjeant, A. A.; Stern, C. L.; Sutter, J.; Meyer, K.; Mirkin, C. A. One-Pot Synthesis of an Fe(II) Bis-Terpyridine Complex with Allosterically Regulated Electronic Properties. *J. Am. Chem. Soc.* **2012**, *134*, 16921−16924.

(24) Dobrawa, R.; Ballester, P.; Saha-Möller, C. R.; Würthner, F. Thermodynamics of 2,2′:6′,2″-Terpyridine-Metal Ion Complexation. In *Metal-Containing and Metallosupramolecular Polymers and Materials*; ACS Symposium Series; American Chemical Society: 2006; Vol. *928*, pp 43−62.

(25) Andres, P. R.; Schubert, U. S. Metallo-Polymerization/-Cyclization of a C16-Bridged Di-Terpyridine Ligand and Iron(II) Ions. *Macromol. Rapid Commun.* **2004**, *25*, 1371−1375.

(26) Li, X.; Chan, Y.-T.; Casiano-Maldonado, M.; Yu, J.; Carri, G. A.; Newkome, G. R.; Wesdemiotis, C. Separation and Characterization of Metallosupramolecular Libraries by Ion Mobility Mass Spectrometry. *Anal. Chem.* **2011**, *83*, 6667−6674.

(27) Newkome, G. R.; Cho, T. J.; Moorefield, C. N.; Cush, R.; Russo, P. S.; Godínez, L. A.; Saunders, M. J.; Mohapatra, P. Hexagonal Terpyridine−Ruthenium and − Iron Macrocyclic Complexes by Stepwise and Self-Assembly Procedures. *Chem. - Eur. J.* **2002**, *8*, 2946−2954.

(28) Perera, S.; Li, X.; Soler, M.; Schultz, A.; Wesdemiotis, C.; Moorefield, C. N.; Newkome, G. R. Hexameric Palladium(II) Terpyridyl Metallomacrocycles: Assembly with 4,4′-Bipyridine and Characterization by TWIM Mass Spectrometry. *Angew. Chem., Int. Ed.* **2010**, *49*, 6539−6544.

DOI: 10.1021/acs.chemmater.7b03638
Chem. Mater. 2017, 29, 10284−10288

(29) Jeon, Y. M.; Heo, J.; Mirkin, C. A. Dynamic interconversion of amorphous microparticles and crystalline rods in salen-based homochiral infinite coordination polymers. *J. Am. Chem. Soc.* **2007**, *129*, 7480−7481.
(30) Ulmann, P. A.; Mirkin, C. A.; DiPasquale, A. G.; Liable-Sands, L. M.; Rheingold, A. L. Reversible Ligand Pairing and Sorting Processes Leading to Heteroligated Palladium(II) Complexes with Hemilabile Ligands. *Organometallics* **2009**, *28*, 1068−1074.

DOI: 10.1021/acs.chemmater.7b03638
Chem. Mater. 2017, 29, 10284−10288

Supporting Information

Infinite Coordination Polymer Particles Composed of Stimuli-Responsive Coordination Complex Subunits

Andrea I. d'Aquino, Zachary S. Kean, Chad A. Mirkin*

*To whom correspondence should be addressed, E-mail: chadnano@northwestern.edu.

Department of Chemistry and International Institute for Nanotechnology, Northwestern University, 2145 Sheridan Road, Evanston, Illinois 60208, United States

Table of Contents

General Methods

All chemicals were purchased from Sigma-Aldrich and used without further purification, unless otherwise stated. (2-chloroethyl)diphenylphosphine[1] and 4'-[4-(mercaptomethyl)phenyl]-2,2':6',2"-terpyridine[2] were synthesized according to literature procedures. Solvents were purchased anhydrous and degassed under a stream of argon prior to use. Flash chromatography was performed using SiliaFlash F60 SiO_2 (230–400 mesh ASTM, 0.040–0.063 mm; SiliCycle). Deuterated solvents were purchased from Cambridge Isotope Laboratories and used as received. ^{1}H and $^{31}P\{^{1}H\}$ NMR spectra were recorded on a Bruker Avance 400 MHz. ^{1}H NMR spectra were referenced to residual proton resonances (CD_2Cl_2 = δ 5.32; CD_3CN = δ 1.94) in the deuterated solvents. ^{13}C NMR spectra were referenced to the solvent peak (CD_2Cl_2 = δ 53.84; CD_3CN = δ 1.32 and 118.26) $^{31}P\{^{1}H\}$ NMR spectra were referenced to an 85% H_3PO_4 aqueous solution. All chemical shifts are reported in ppm. High resolution mass spectra measurements (HR-MS) were recorded on an Agilent 6120 LC-TOF instrument in positive ion mode. Transmission electron microscopy (TEM) imaging and energy dispersive X-ray data were performed and collected on a Hitachi HD-2300 STEM microscope operating at 200 kV, equipped with two Thermo Scientific Energy Dispersive X-ray (EDX) detectors. TEM samples were prepared by drop-casting a 5 µL Et_2O solution of particles onto a carbon-coated Cu TEM grid (Ted Pella). Single crystals suitable for X-ray diffraction studies were mounted using oil (Infineum V8512) on a glass fiber. All measurements were made on a CCD area detector with graphite monochromated Mo Kα or Cu Kα radiation. Data were collected using Bruker APEXII detector and processed using APEX2 from Bruker. Dynamic light scattering (DLS) data were collected using a Zetasizer Nano ZS (Malvern Instruments Ltd). All XRD structures were solved by direct methods and expanded using Fourier techniques. The non-hydrogen atoms were refined anisotropically. Hydrogen atoms were included in idealized positions, but not refined. Their positions were constrained relative to their parent atom.

Synthetic Methods

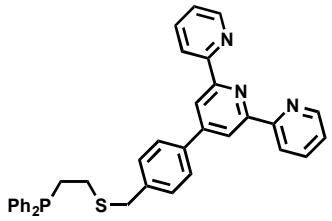

1

4'-[4-(mercaptomethyl)phenyl]-2,2':6',2"-terpyridine was prepared according to literature procedures.[2a,b] In a glove box: 4'-[4-(mercaptomethyl)phenyl]-2,2':6',2"-terpyridine (475 mg, 1.34 mmol) was transferred to a 6 mL vial with stir bar and dissolved in 7 mL CH_3CN. Potassium *tert*-butoxide (150 mg, 1.34 mmol) in 2 mL THF was added slowly while stirring rapidly to produce a light yellow suspension. (2-chloroethyl)diphenylphosphine (367 mg, 1.47 mmol) was then added as a solid and the vial was sealed, removed from the glovebox, and allowed to stir at 70 °C overnight. The solution was cooled, then passed through a short plug of neutral alumina, which was washed with an additional 50 mL of CH_2Cl_2. The solvent was removed under reduced pressure and the residue was recrystallized from CH_2Cl_2/EtOH to give **1** as fine white needles (530 mg) in 70 % yield.

^{1}H NMR (400 MHz, CD_2Cl_2): δ = 8.76 (s, 2H), 8.73 (m, 2H), 8.70 (m, 2H), 7.91 (td, *J* = 7.7, 1.8 Hz, 2H), 7.79 (d, *J* = 8.2 Hz, 2H), 7.38 (m, 8H), 7.33 (m, 6H), 3.79 (s, 2H), 2.52 (m, 2H), 2.31 (m, 2H). ^{13}C{^{1}H} NMR (101 MHz, CD_2Cl_2): δ = 156.51, 156.41, 150.11, 149.58, 140.10, 138.51 (d, J_{C-P} = 13.9 Hz), 137.54, 137.23, 133.05 (d, J_{C-P} = 18.8 Hz), 129.89, 129.12, 128.90 (d, J_{C-P} = 6.6 Hz), 127.69, 124.29, 121.48, 118.97, 36.22, 28.86 (d, J_{C-P} = 15.1 Hz), 28.08 (d, J_{C-P} = 21.6 Hz). ^{31}P{^{1}H} NMR (162 MHz, CD_2Cl_2): δ = -17.05. ESI-HRMS (m/z): Calcd: 568.1971 [M+H]+. Found: 568.1982.

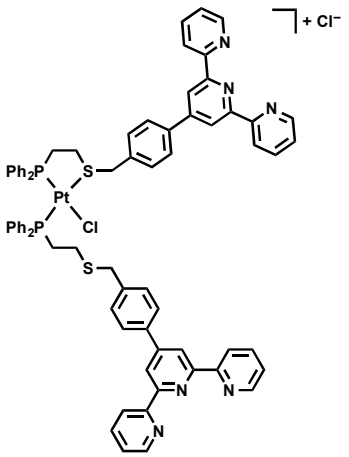

2-Pt-Open

Dichloro(1,5-cyclooctadiene)platinum(II) ($Pt(COD)Cl_2$, 65.8 mg, 0.176 mmol) was weighed into a 6 mL vial with a stir bar and 2 mL of CH_2Cl_2 was added. A solution of **1** (200 mg, 0.352 mmol) in 2 mL CH_2Cl_2 was prepared and added dropwise to the mixture containing $Pt(COD)Cl_2$ while stirring. After 10 min, the homogenous clear solution was evaporated under reduced pressure to a minimal volume and Et_2O was added to precipitate a white solid. The solid was collected by centrifugation, redissolved in CH_2Cl_2, and precipitated into Et_2O to yield **2-Pt-Open** as a microcrystalline white solid in quantitative yield.

^1H NMR (400 MHz, CD_2Cl_2): δ = 8.72 (s, 4H), 8.71 (m, 4H), 8.68 (m, 4H), 7.90 (td, J = 7.7, 1.8 Hz, 4H), 7.69 (d, J = 8.2 Hz, 4H), 7.62 (d, J = 7.8 Hz, 4H), 7.51 (t, J = 7.3 Hz, 4H), 7.39–7.21 (m, 20H), 4.42 (br s, 4H), 2.74 (br m, 8H). $^{31}P\{^1H\}$ NMR (162 MHz, T = 193 K, CD_2Cl_2): δ = 42.66 (J_{P-Pt} = 3595 Hz), 6.98 (J_{P-Pt} = 3105 Hz). ESI-HRMS (m/z): Calcd: 1365.3132 [M–Cl]+. Found: 1365.3129

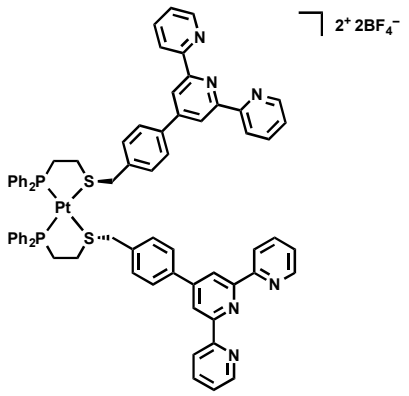

2-Pt-Closed

Thallium tetrafluoroborate ($TlBF_4$, 23 mg, 0.079 mmol) was weighed into a 2 mL vial equipped with a stir bar and 1 mL of CH_3CN was added. With stirring, **1** (54 mg, 0.039 mmol) was added as a solution in CH_2Cl_2 (4 mL) and allowed to react for 30 min. The white suspension was then filtered through celite and washed with an excess of CH_2Cl_2 to give a translucent light yellow solution. The solution was evaporated under reduced pressure and redissolved in 3 mL of CH_2Cl_2 to give a slightly cloudy suspension that was filtered through a 0.2 μm PTFE filter. The resulting solution was then evaporated under reduced pressure to give **2-Pt-Closed** (57 mg) as a yellow microcrystalline solid in 98 % yield.

^{1}H NMR (400 MHz, CD_3CN): δ = 8.60 (m, 4H), 8.57 (s, 4H), 8.54 (dt, J = 7.9, 1.1, 4H), 7.90 (d, J = 8.0 Hz, 4H), 7.88 (td, J = 7.9, 1.8 Hz, 4H), 7.66 (d, J = 8.3 Hz, 4H), 7.60–7.10 (br, 20H) 7.36 (ddd, J = 7.5, 4.8, 1.2 Hz, 4H), 4.68 (br s, 4H), 2.98 (br m, 8H). ^{31}P{^{1}H} NMR (162 MHz, CD_3CN): δ = 46.91 ($J_{P–Pt}$ = 3032 Hz). ESI-HRMS (m/z): Calcd: 1417.3473 [M–BF_4]+. Found: 1417.3505.

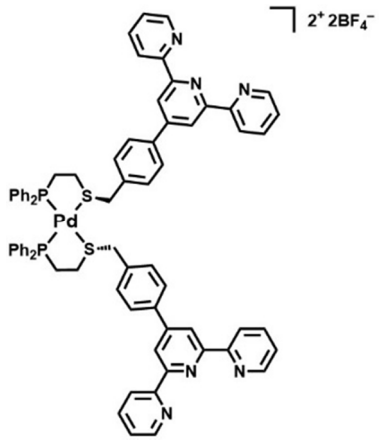

2-Pd-Closed

In the glovebox, tetrakis(acetonitrile)palladium(II) tetrafluoroborate ($Pd(MeCN)_4(BF_4)_2$, 39.2 mg, 0.088 mmol) was weighed into a 6 mL vial with a stir bar and 2 mL of CH_2Cl_2 was added. A solution of **1** (100 mg, 0.176 mmol) in 2 mL CH_2Cl_2 was prepared and added dropwise to the mixture containing $Pd(MeCN)_4(BF_4)_2$ while stirring. After 10 min, the homogenous clear, yellow solution was evaporated under reduced pressure to a minimal volume and Et_2O was added to precipitate a yellow solid. The solid was collected by centrifugation, redissolved in CH_2Cl_2, and precipitated into Et_2O to yield **2-Pd-Closed** (133 mg) as a microcrystalline yellow solid in quantitative yield.

^1H NMR (400 MHz, CD_2Cl_2): δ = 8.60 (m, 2H), 8.59 (m, 2H), 8.58 (s, 4H), 8.56 (d, J = 1.14, 2H), 8.54 (d, J = 1.07, 2H), 7.86 (s, 2H), 7.84 (s, 2H), 7.79 (td, J = 7.78, 1.4, 4H), 7.55 (m, 9H), 7.47 (br m, 15H), 7.25 (ddd, J = 7.45, 4.72, 1.20, 4H), 4.54 (s, 4H), 3.37 (dq, J = 10.41, 6.33, 5.85, 4H). $^{31}P\{^1H\}$ NMR (162 MHz, CD_2Cl_2): δ = 61.58. ESI-HRMS (m/z): Calcd: 1327.2890 $[M–BF_4]+$. Found: 1327.2875

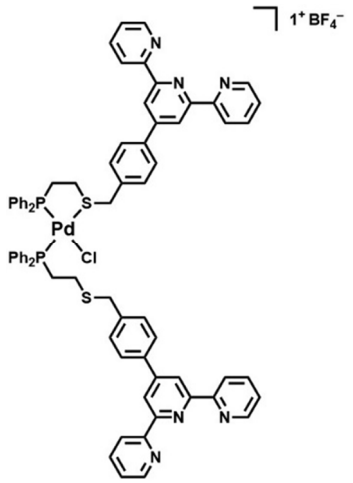

2-Pd-Open

2-Pd-Open was synthesized via two different procedures:

1. Chloride salt method: In a dry 6 mL vial equipped with a stir bar, **2-Pd-Closed** was dissolved in ~2 mL of CH_2Cl_2 and allowed to dissolve. In a separate vial, a solution of tetrabutylammonium chloride (8 mg, 0.029 mmol) was prepared in CH_2Cl_2 and added to the solution of **2-Pd-Closed** and allowed to react for 30 min. The resulting homogeneous, clear, yellow solution was then evaporated under reduced pressure to give **2-Pd-Open** as a yellow microcrystalline solid in quantitative yield.
2. Chloride resin method: **2-Pd-Closed** was measured into a falcon tube (12 mg, 0.008 mmol) and dissolved in 2 mL of CH_3CN. In a separate falcon tube, 312 mg of Dowex 1x4 chloride resin (100-200 mesh) was measured out and mixed with 3 mL of CH_3CN. The solution containing **2-Pd-Closed** was slowly transferred (via pipette) to the flacon tube containing the Dowex chloride resin. Once completely transferred, the solution was mixed continuously for 30 min. After 30 min, solution was filtered and the resin washed with 1 mL portions of CH_3CN. The resulting homogeneous, clear, yellow solution was then evaporated under reduced pressure to give **2-Pd-Open** as a yellow microcrystalline solid in 88% yield.

^{1}H NMR (400 MHz, CD_3CN): δ = 8.67 (m, 13H), 7.89 (td, J = 7.76, 1.82, 4H), 7.67 (d, J = 7.99, 4H), 7.54 (m, 8H), 7.36 (m, 12H), 7.19 (dd, J = 12.40, 7.73, 8H), 4.23 (s, 4H), 3.14 (m, 9 H), 2.74 (m, 4H), 2.56 (m, 4H). ^{31}P{^{1}H} NMR (162 MHz, CD_3CN): δ = 65.06, 43.34. ESI-HRMS (m/z): Calcd: 1365.3186 [M–BF_4]+. Found: 1365.3146.

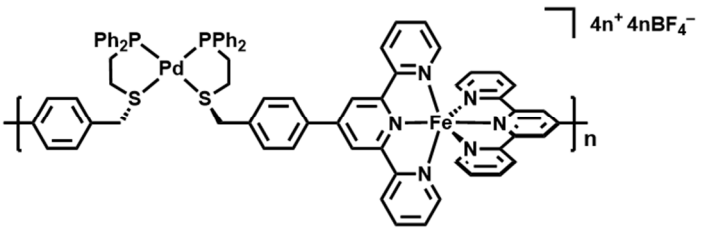

3-Pd-Closed

A solution of iron(II)tetrafluoroborate hexahydrate ($Fe(BF_4)_2$•$6H_2O$) was prepared by dissolving 0.0040 g of $Fe(BF_4)_2$•$6H_2O$ in 500 µL of CD_3CN. The prepared $Fe(BF_4)_2$•$6H_2O$ solution was then added to a solution of **2-Pd-Closed** (9.8 mg, 0.007 mmol) in CD_3CN until a 1:1 molar ratio was achieved (2.3 mg of $Fe(BF_4)_2$, 0.007 mmol). The solution changed from a clear, yellow solution to a dark purple solution.

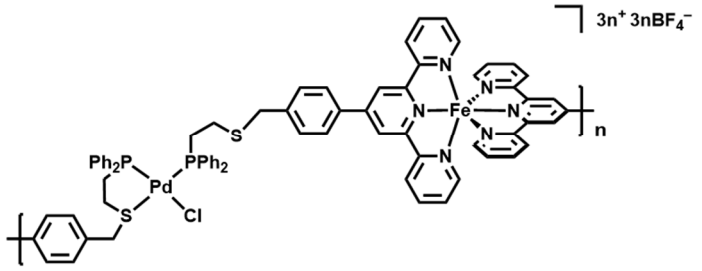

3-Pd-Open

3-Pd-Open can be prepared from **2-Pd-Open** prepared by either of the two outlined procedures, above. A solution of iron(II)tetrafluoroborate hexahydrate ($Fe(BF_4)_2$•$6H_2O$) was prepared by dissolving 0.0041 g of $Fe(BF_4)_2$•$6H_2O$ in 200 µL of CD_3CN. The prepared $Fe(BF_4)_2$•$6H_2O$ solution was then added into a solution of **2-Pd-Open** (12.0 mg, 0.009 mmol) in CD_3CN until a 1:1 molar ratio was achieved (3.0 mg of $Fe(BF_4)_2$, 0.009 mmol) The solution changed from a clear, yellow solution to a dark purple solution.

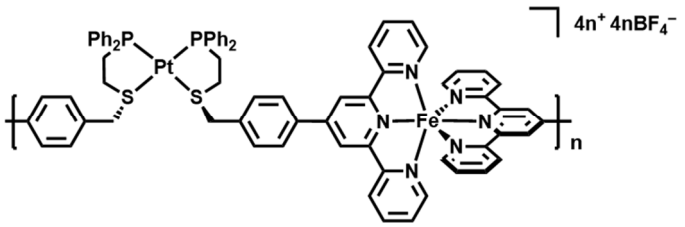

3-Pt-Closed

A solution of iron(II)tetrafluoroborate hexahydrate ($Fe(BF_4)_2$•$6H_2O$) was prepared by dissolving 0.0040 g of $Fe(BF_4)_2$•$6H_2O$ in 200 µL of CD_3CN. The prepared $Fe(BF_4)_2$•$6H_2O$ solution was then added to a solution of **2-Pt-Closed** (3.0 mg, 0.002 mmol) in CD_3CN until a 1:1 molar ratio was achieved (0.673 mg of $Fe(BF_4)_2$, 0.002 mmol). The solution changed from a clear, yellow solution to a dark purple solution.

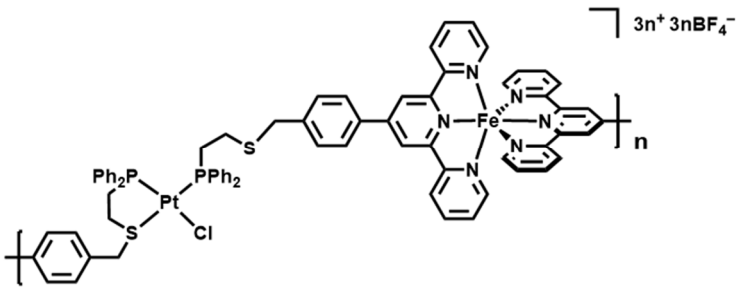

3-Pt-Open

A solution of iron(II)tetrafluoroborate hexahydrate ($Fe(BF_4)_2$•$6H_2O$) was prepared by dissolving 0.0040 g of $Fe(BF_4)_2$•$6H_2O$ in 300 µL of CD_3CN. The prepared $Fe(BF_4)_2$•$6H_2O$ solution was then added to a solution of **2-Pt-Open** (6.0 mg, 0.004 mmol) in CD_3CN until a 1:1 molar ratio was achieved (1.44 mg of $Fe(BF_4)_2$, 0.004 mmol). The solution changed from a clear, yellow solution to a dark purple solution.

X-ray Crystal Data

A

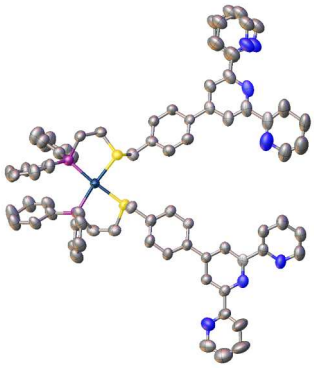

B

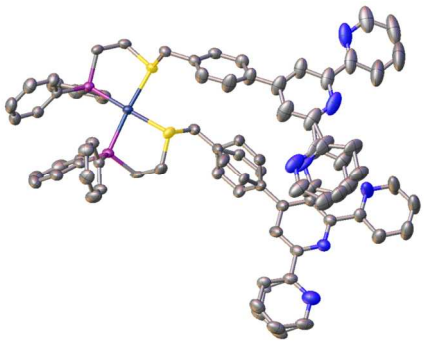

Figure S1. Crystal structures of (a) **2-Pt-Closed** (obtained from the slow diffusion of ether into acetonitrile) and (b) the **2-Pd-Closed** (obtained from the slow diffusion of ether into DCM) drawn with 50% thermal ellipsoid probability. Hydrogen atoms, solvent molecules, and anions have been omitted for clarity.

Table S1. Crystal data and structural refinement for **2-Pt-Closed and 2-Pd-Closed**.

	2-Pt-Closed	**2-Pd-Closed**
Empirical formula	$C_{72}H_{60}F_{18}N_6P_5PtS_2$	$C_{76}H_{70}B_2F_8N_6OP_2PdS_2$
Formula weight	1765.32	1489.46
Temperature / K	100.0	149.99
Crystal system	orthorhombic	monoclinic
Space group	Ccce	$P2_1/c$
a / Å	22.614(4)	9.5073(5)
b / Å	28.042(5)	35.1644(18)
c / Å	54.989(12)	21.6818(11)
α/°	90	90
β/°	90	92.515(4)
γ/°	90	90
Volume / $Å^3$	34871(12)	7241.6(6)
Z	16	4
ρ_{calc} / mg mm^{-3}	1.345	1.366
μ / mm^{-1}	5.013	3.601

F(000)	14096	3064.0
Crystal size / mm^3	0.222 × 0.146 × 0.014	0.259 × 0.095 × 0.006
2Θ range for data collection	3.214 to 127.094°	5.026 to 136.634°
Index ranges	$0 \le h \le 25$, $0 \le k \le 32$, $0 \le l \le 63$	$-11 \le h \le 10$, $-42 \le k \le 40$, $-18 \le l \le 26$
Reflections collected	12624	34154
Independent reflections	12007[R(int) = 0.0000]	12892[R(int) = 0.0642]
Data/restraints/parameters	12007/1119/982	12892/534/1033
Goodness-of-fit on F^2	1.046	1.050
Final R indexes [$I>2\sigma(I)$]	$R_1 = 0.0965$, $wR_2 = 0.2614$	$R_1 = 0.0605$, $wR_2 = 0.1515$
Final R indexes [all data]	$R_1 = 0.1278$, $wR_2 = 0.2786$	$R_1 = 0.0803$, $wR_2 = 0.1607$
Largest diff. peak/hole / e $Å^{-3}$	1.502/-0.786	0.939/-0.938

Characterization of Coordination-Polymers Bearing WLA Subunits

In order to determine the stoichiometry of metal-ligand binding, we conducted a titration wherein samples each containing a fixed concentration of 230 μM **2-M-Open** or **2-M-Closed** (M = Pd^{II} or Pt^{II}) in 1 mL CD_3CN were prepared with increasing amounts of $Fe(BF_4)_2 \cdot 6H_2O$ ranging from 0 to 300 μM.

^{1}H NMR and ^{1}H DOSY Spectra of Coordination Polymers

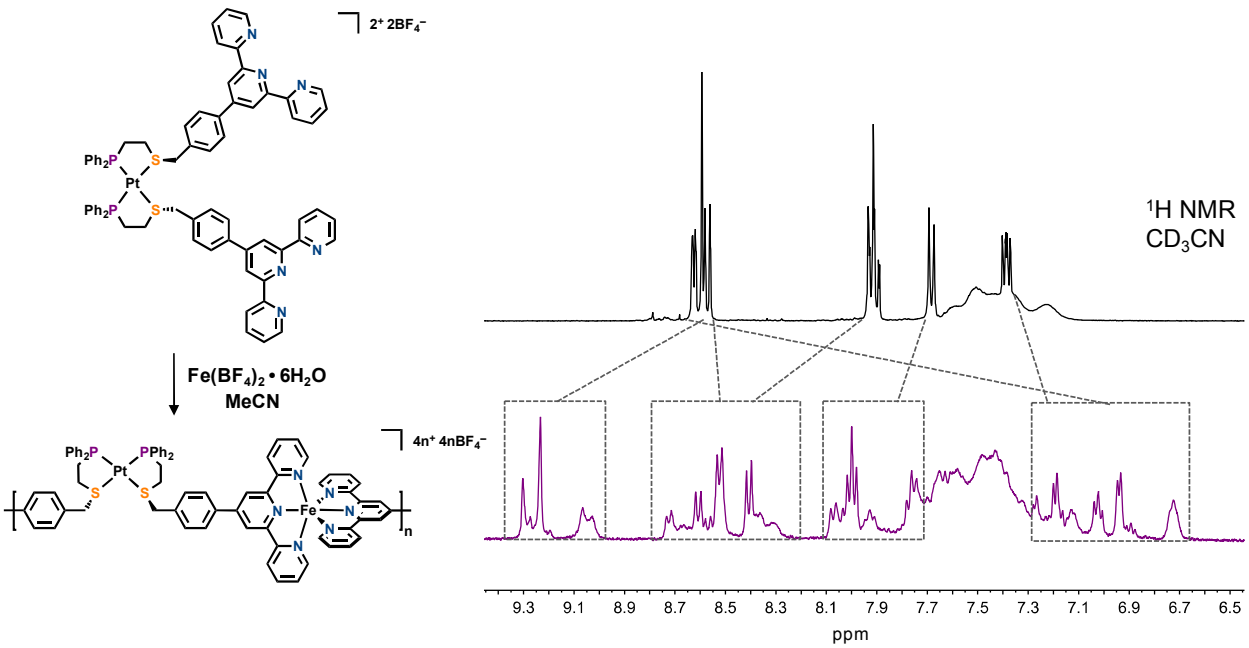

Figure S2. ^{1}H NMR spectra of monomer **2-Pt-Closed** before (top) and after (bottom) the addition of one equivalent of $Fe(BF_4)_2 \cdot 6H_2O$ to form **3-Pt-Closed**. Dashed lines and boxes show free terpyridine resonances shifting to regions indicative of iron binding.[3]

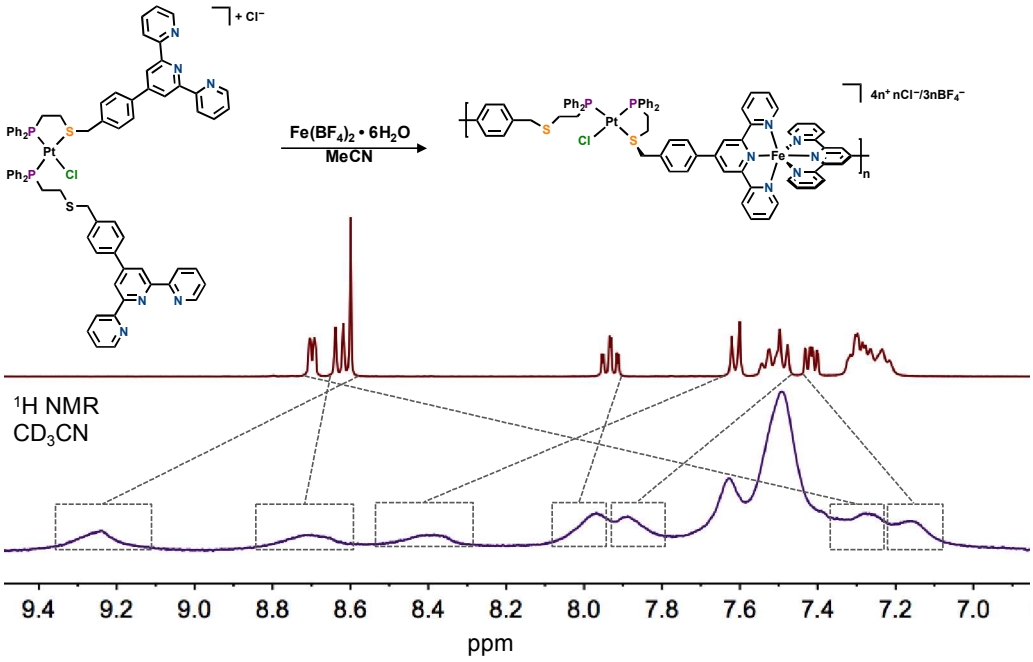

Figure S3. ^{1}H NMR spectra of monomer **2-Pt-Open** before (top) and after (bottom) the addition of one equivalent of $Fe(BF_4)_2$•$6H_2O$ to form **3-Pt-Open**. Dashed lines and boxes show free terpyridine resonances shifting to regions indicative of iron binding.[3]

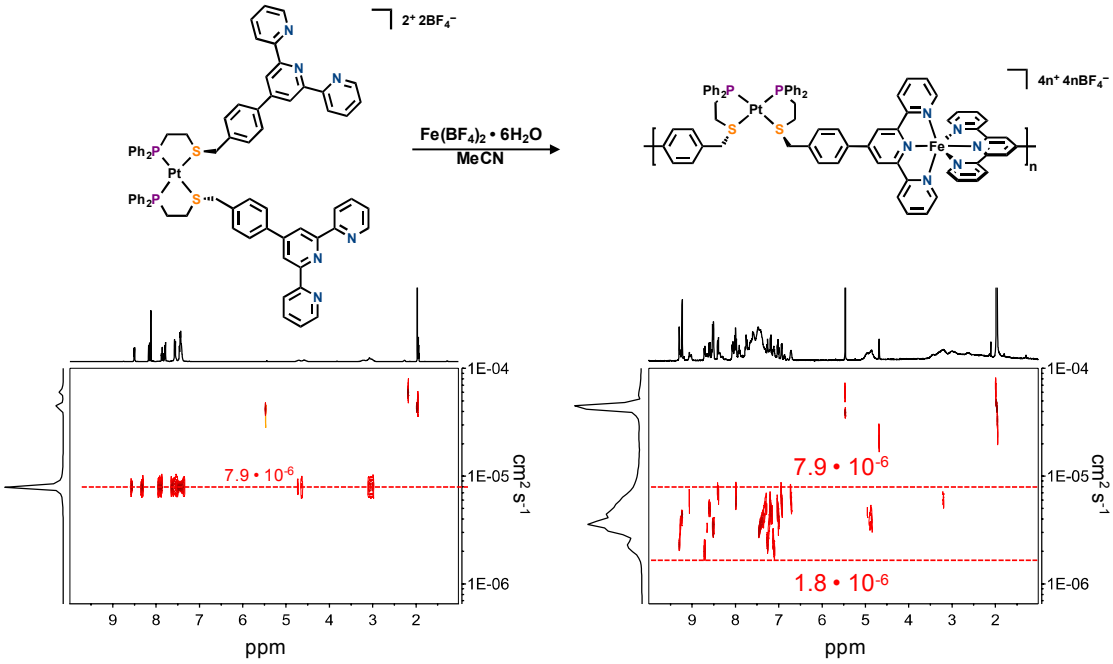

Figure S4. ^{1}H DOSY NMR spectra of monomer **2-Pt-Closed** (D = 7.9 • 10^{-6} cm^2s^{-1}) before (left) and after (right) the addition of $Fe(BF_4)_2$•$6H_2O$ to form **3-Pt-Closed**. The Spectrum of **3-Pt-Closed** indicates the complete consumption of the starting monomer and the formation of oligomeric species with diffusion coefficients reduced by up to a factor of four.

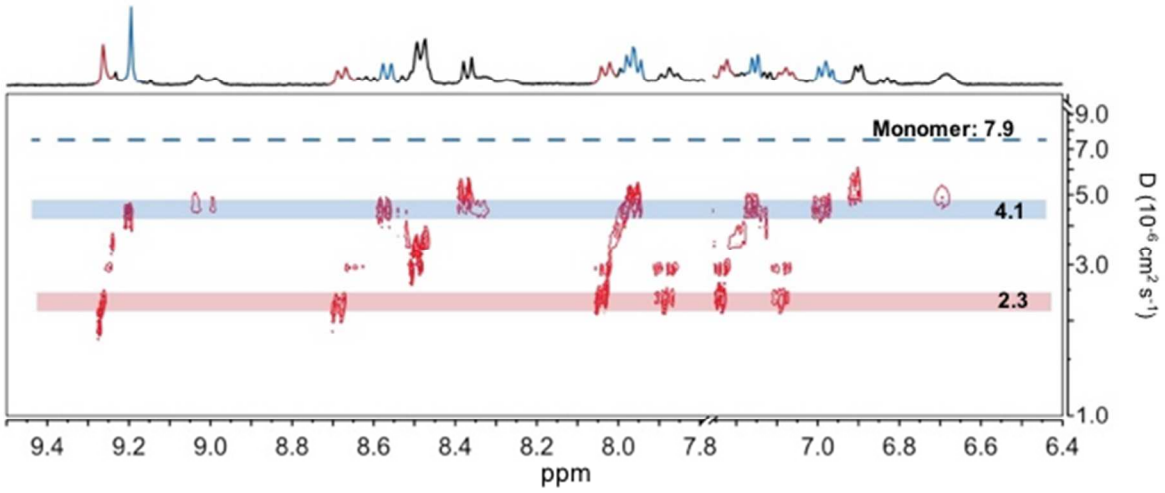

Figure S5. ^{1}H DOSY NMR spectra of monomer **2-Pt-Closed** (D = 7.9 • 10^{-6} cm^2s^{-1}) before (left) and after (right) the addition of $Fe(BF_4)_2$•$6H_2O$ to form **3-Pt-Closed**. The Spectrum of **3-Pt-Closed** indicates the complete consumption of the starting monomer and the formation of oligomeric species with diffusion coefficients reduced by up to a factor of four.

DFT Calculations

All calculations were carried out with the use of SCM's Amsterdam Density Functional (ADF2016.104) suite on a 12-core computational cluster. The model for **3-Pd-Closed** and **3-Pt-Closed** were built ignoring counter anions and assuming local charge(s) arising from the Pd(II) or Pt(II) metal center only. Geometry optimizations of all electrons were made by applying the generalized gradient approximation method (GGA) with bases sets containing triple-ζ functions with two polarization functions (TZ2P), and the local density approximation of Becke, Perdew and Ernzerhof (PBE).[4] Scalar relativistic effects were taken into consideration for heavy metal atoms.

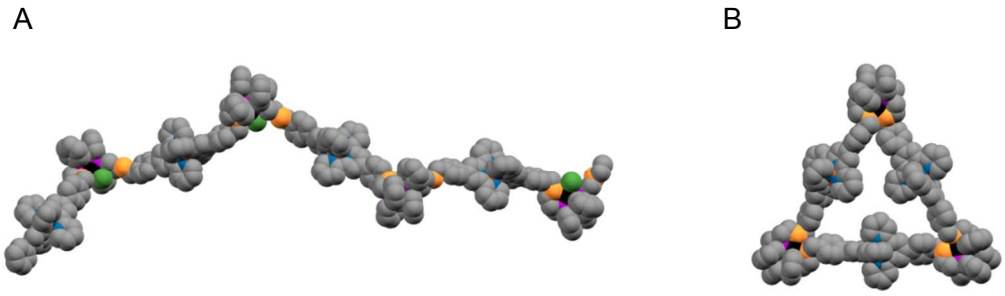

Figure S6. Density function theory (DFT) energy minimized models of A) **3-Pd-Closed** and B) **3-Pt-Closed**. The lowest energy conformation of **3-Pt-Closed** resembles cyclic oligomers.

Post-Polymerization Switching of States

In order to switch from the closed Pd^{II} coordination polymer (**3-Pd-Closed**) to the open Pd^{II} coordination polymer (**3-Pd-Open**), a solution of **3-Pd-Closed** (10 mg, 0.007 mmol) in CH_3CN was treated with tetrabutylammonium chloride (TBAC, 2 mg, 0.007 mmol). The solution was filtered, and the resulting homogeneous, clear, purple solution was evaporated under reduced pressure to give **3-Pd-Closed**. In order to switch from the open Pd^{II} coordination polymer (**3-Pd-Open**) to the closed Pd^{II} coordination polymer (**3-Pd-Closed**), **3-Pd-Closed** (25 mg, 0.018 mmol) was dissolved in ~4 mL of CH_3CN in a falcon tube. In a separate falcon tube, 440 mg of Dowex 1x4 chloride resin (100-200 mesh) was measured out and mixed with 4 mL of CH_3CN. The solution containing **3-Pd-Closed** was slowly transferred (via pipette) to the falcon tube containing the Dowex chloride resin. Once completely transferred, the solution was mixed continuously for 30 min. After 30 min, the solution was filtered, and the resin was washed with 1 mL portions of CH_3CN. The filtrate was collected, and the resulting homogeneous, clear, purple solution was then evaporated under reduced pressure to give **3-Pd-Open**.

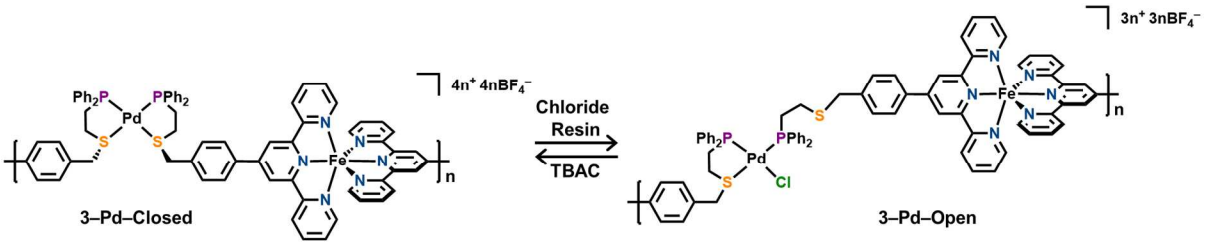

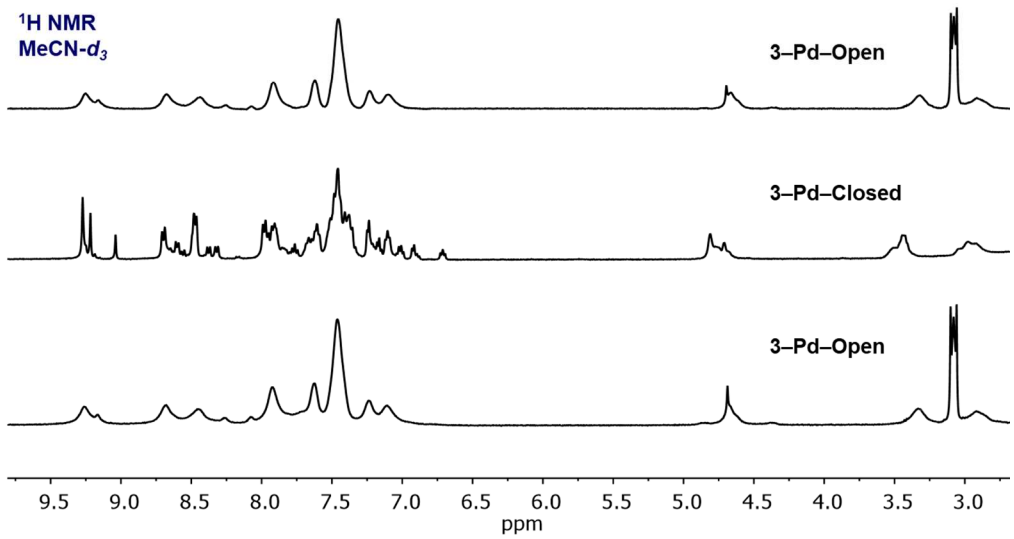

Figure S7. ^{1}H NMR spectra of coordination polymer **3-Pd-Open** (bottom) converted to **3-Pd-closed** (middle) *via* abstraction of chloride post-polymerization, and **3-Pd-closed** (middle)

switched to **3-Pd-Open** (top) *via* addition of chloride post polymerization. All NMR spectra were taken in CD_3CN.

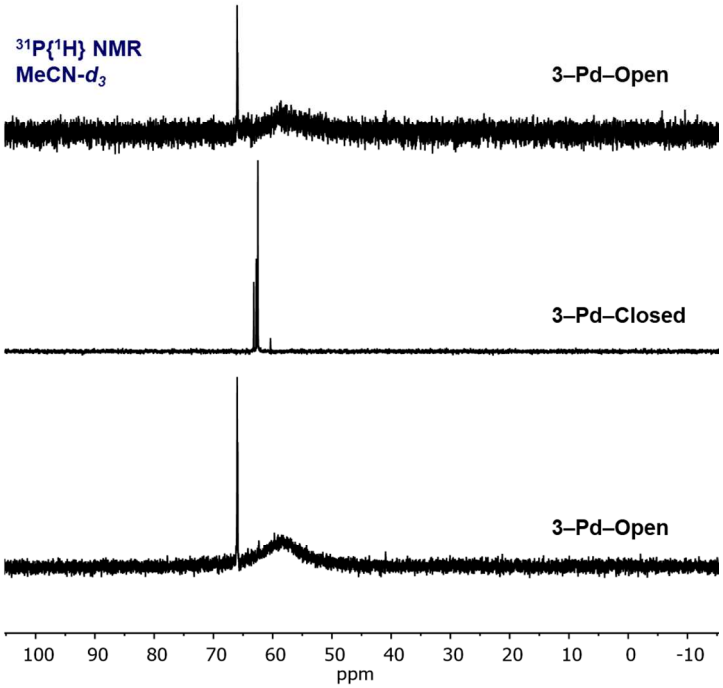

Figure S8. $^{31}P\{^1H\}$ NMR spectra of coordination polymer **3-Pd-Open** (bottom) converted to **3-Pd-closed** (middle) *via* abstraction of chloride post-polymerization, and **3-Pd-closed** (middle) switched to **3-Pd-Open** (top) *via* addition of chloride post polymerization. All NMR spectra were taken in CD_3CN.

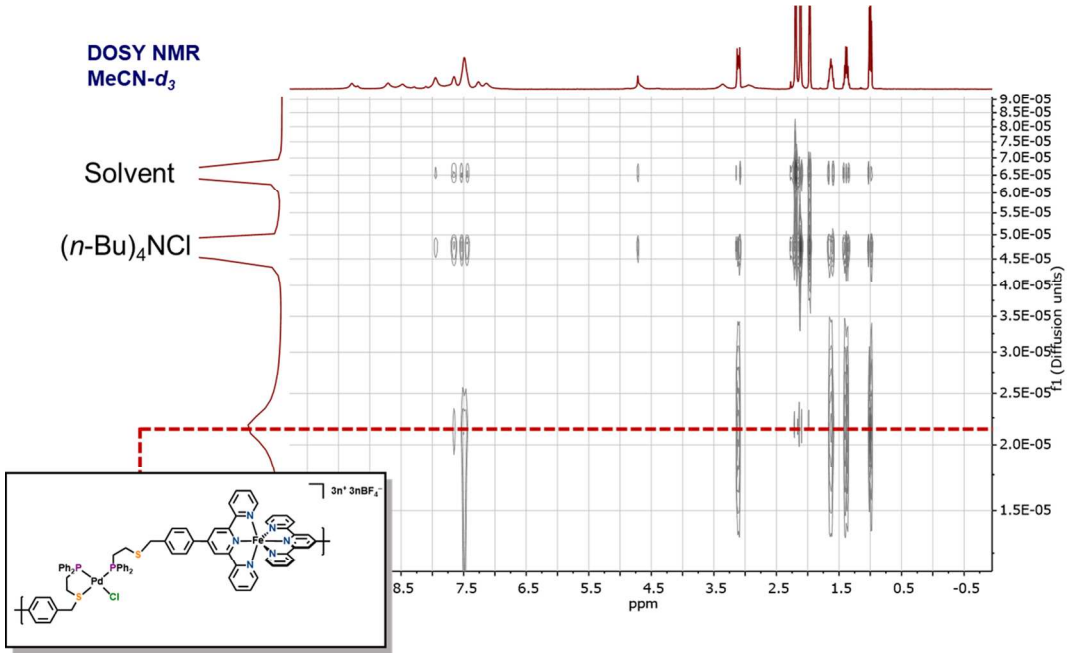

Figure S9. ^{1}H DOSY spectrum, taken in CD_3CN, of resulting **3-Pd-Open** from **3-Pd-Closed**, indicating the formation of one polymeric species.

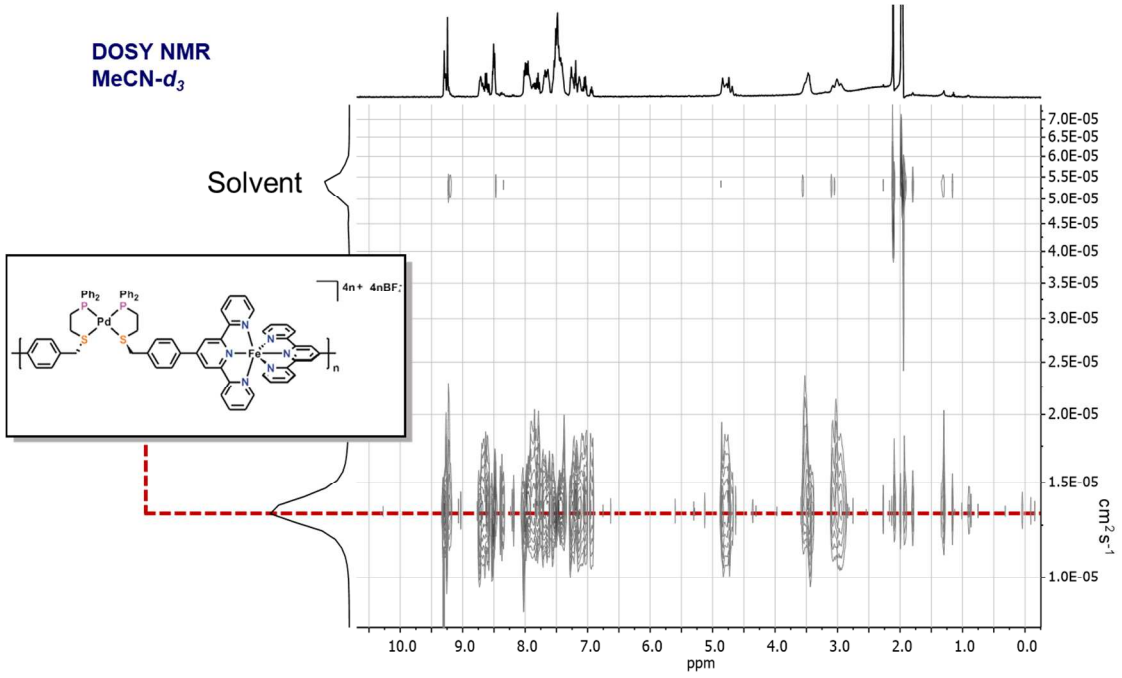

Figure S10. ^{1}H DOSY spectrum, taken in CD_3CN, of resulting **3-Pd-Closed** from **3-Pd-Open**, indicating the formation of one polymeric species.

In order to switch from **3-Pt-Closed** to **3-Pt-Open**, **3-Pt-Closed** (9 mg, 0.006 mmol) was dissolved in ~3 mL of CH_3CN in a falcon tube. In a separate falcon tube, 300 mg of Dowex 1x4 chloride resin (100-200 mesh) was measured out and mixed with 3 mL of CH_3CN. The solution containing **3-Pt-Closed** was slowly transferred (via pipette) to the flacon tube containing the Dowex chloride resin. Once completely transferred, the solution was stirred continuously for 30 min. After 30 min, the solution was filtered, and the resin was washed with 1 mL portions of CH_3CN. Switching from **3-Pt-Open** to **3-Pt-Closed** was achieved by dissolving **3-Pt-Open** (6 mg, 0.004 mmol) in CH_3CN and treating it with $TlBF_4$ (1.2 mg, 0.004 mmol) and the mixture was stirred for one hour.

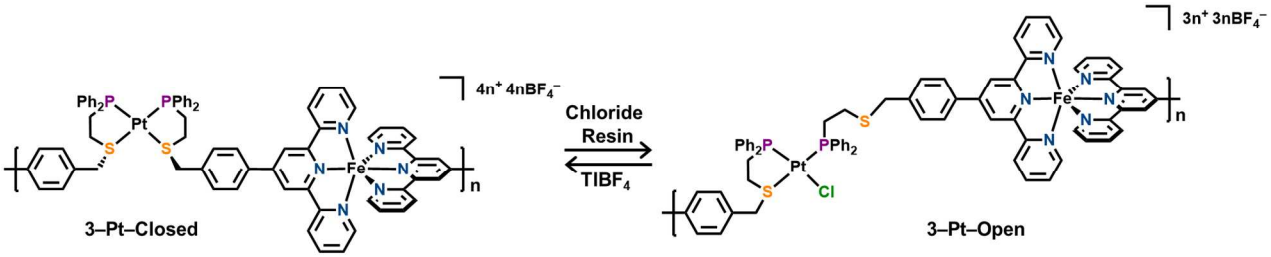

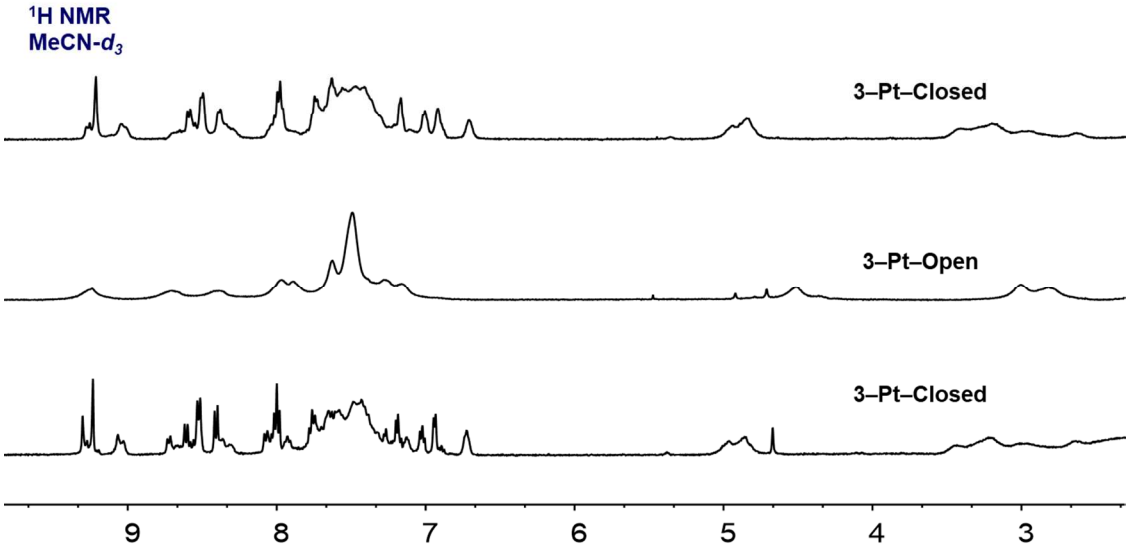

Figure S11. ^{1}H NMR spectra of coordination polymer **3-Pt-Closed** (bottom) converted to **3-Pt-Open** (middle) *via* addition of chloride post-polymerization, and **3-Pt-Open** (middle) switched to **3-Pt-Closed** (top) *via* abstraction of chloride post polymerization. All NMR spectra were taken in CD_3CN.

Infinite Coordination Polymer Particle Characterization

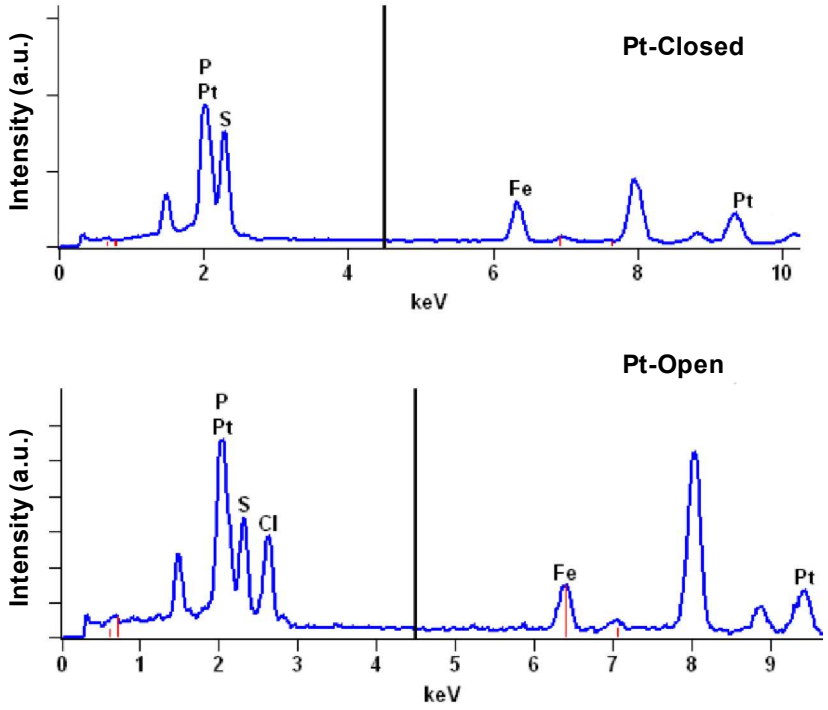

Figure S12. Representative EDS spectra for ICPs composed of **3-Pt-Closed** (top) and **3-Pt-Open** (bottom) showing the presence of Cl, which is indicative of the fully open complex.

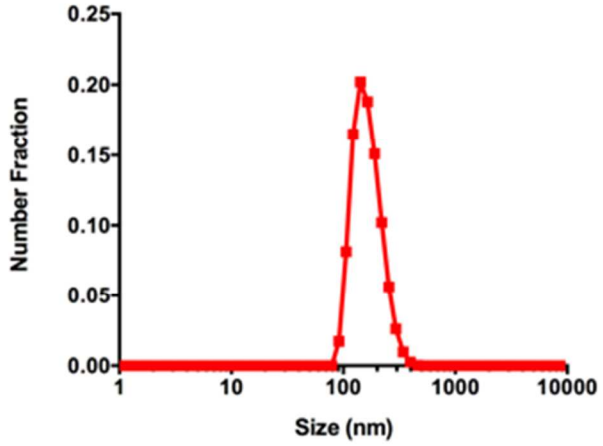

Figure S13. Representative DLS trace for colloidally stable ICPs composed of **3-Pt-Open** synthesized from a 2 mM solution (Diameter$_{\text{number average}}$ = 164 nm, Diameter$_{\text{Z-average}}$ = 195 nm, PDI = 0.089).

ICP Particles Synthesis in Varying Conditions

ICP particles composed of **3-Pt-Closed** were prepared with sub-stoichiometric equivalents of chloride, and the resulting particle morphologies were analyzed using STEM. A solution of **3-Pt-Closed** (12 mg, 0.008 mmol) was dissolved in 4 mL of CH_3CN and tetrabutylammonium chloride (1.1 mg, 0.004 mmol) was added. Particles were synthesized from 8 mM solutions (with respect to the monomer).

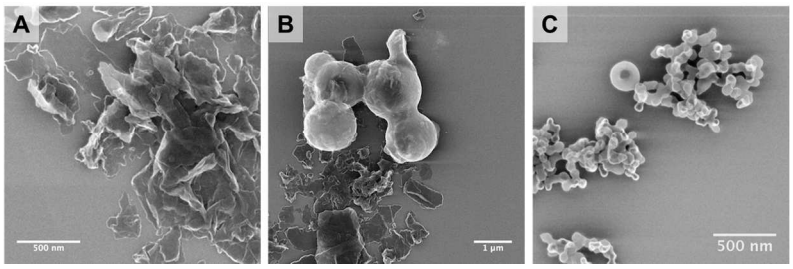

Figure S14. ICP particles composed of **3-Pt-Closed** containing A) 0 equiv. of chloride, B) 0.5 equiv. of chloride, and C) 1 equiv. of chloride.

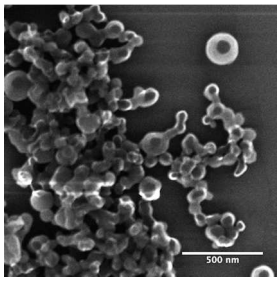

Figure S15. ICP particle synthesis from a 2 mM solution of **3-Pt-Closed**, at ~5 °C, resulting in ill-defined aggregates of small spheres.

NMR Spectra

^{1}H NMR and ^{31}P{^{1}H} NMR of: Ligand 1

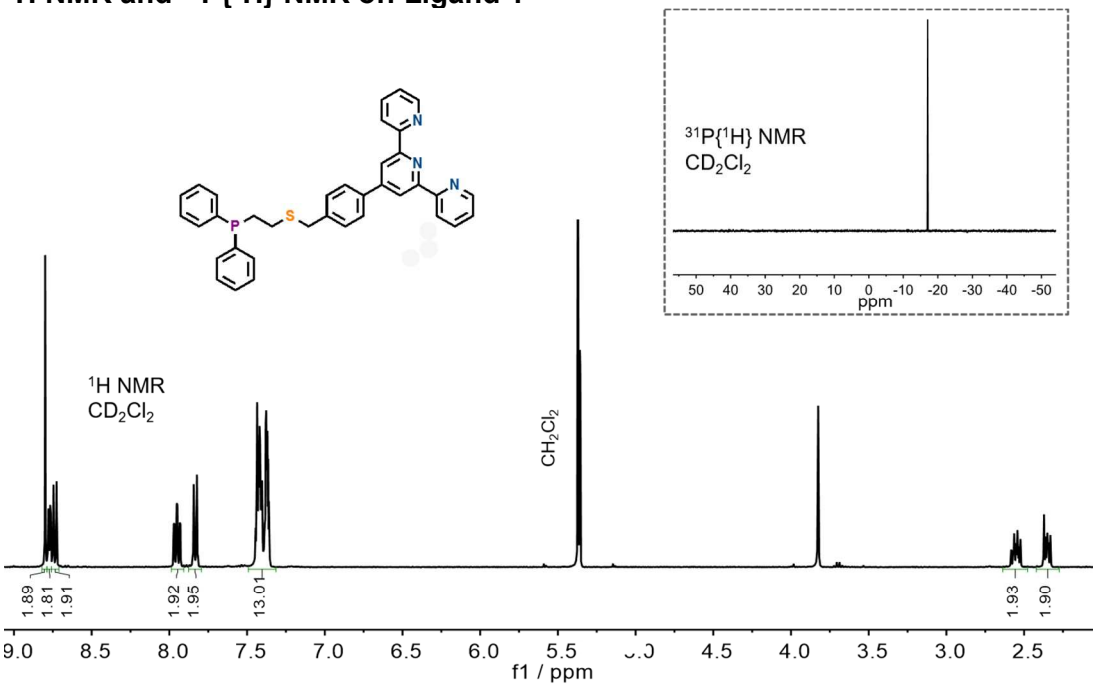

^{1}H NMR and ^{31}P{^{1}H} VT NMR of: 2-Pt-Open

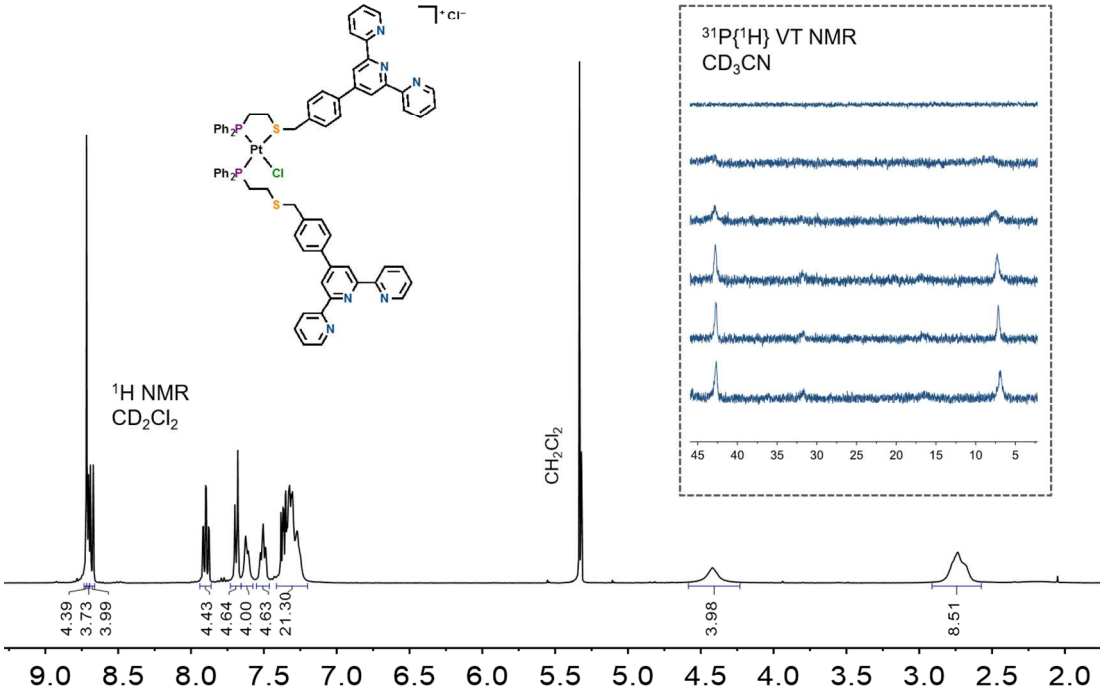

^{1}H NMR and ^{31}P{^{1}H} NMR of: 2-Pt-Closed

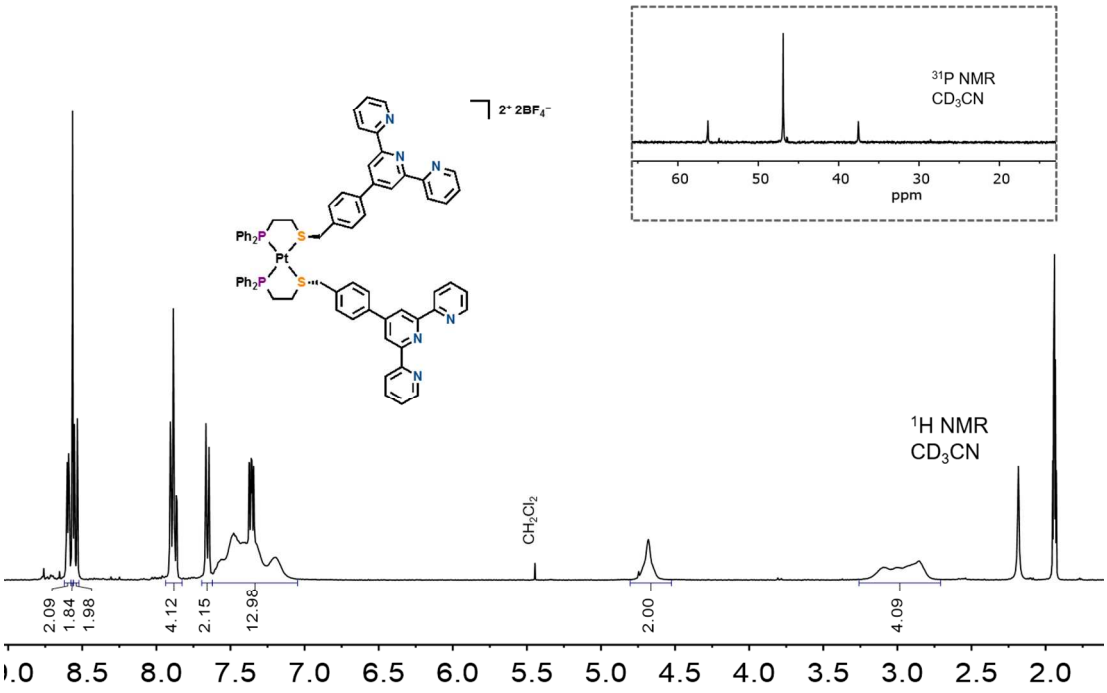

^{1}H NMR and ^{31}P{^{1}H} NMR of: 2-Pd-Closed

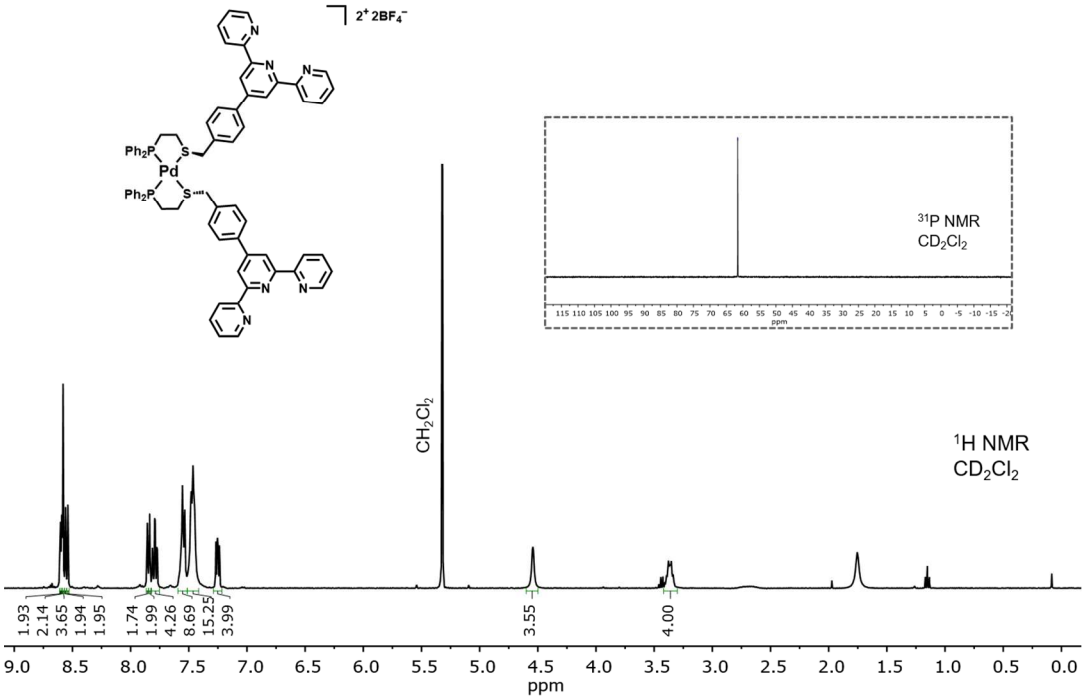

^{1}H NMR and $^{31}P\{^{1}H\}$ NMR of: 2-Pd-Open

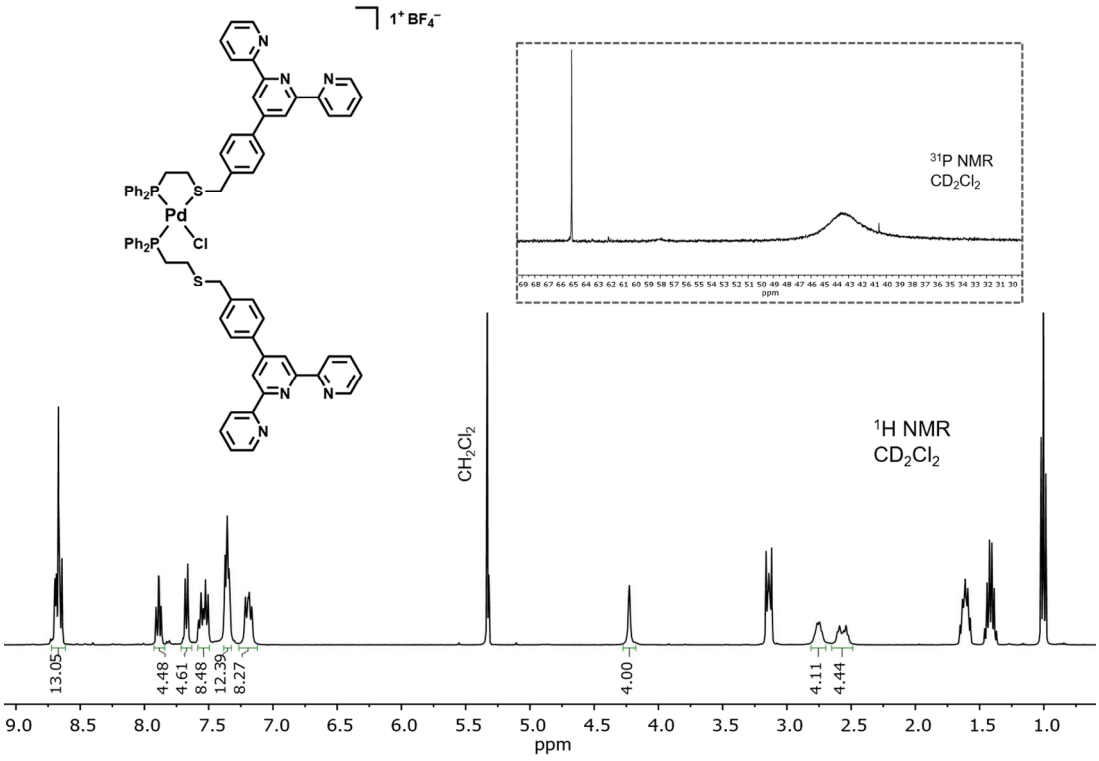

Mass Spectra

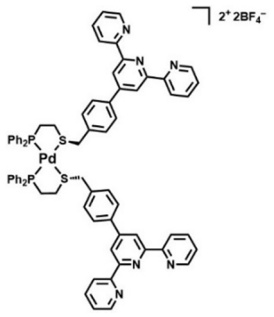

2-Pd-Closed

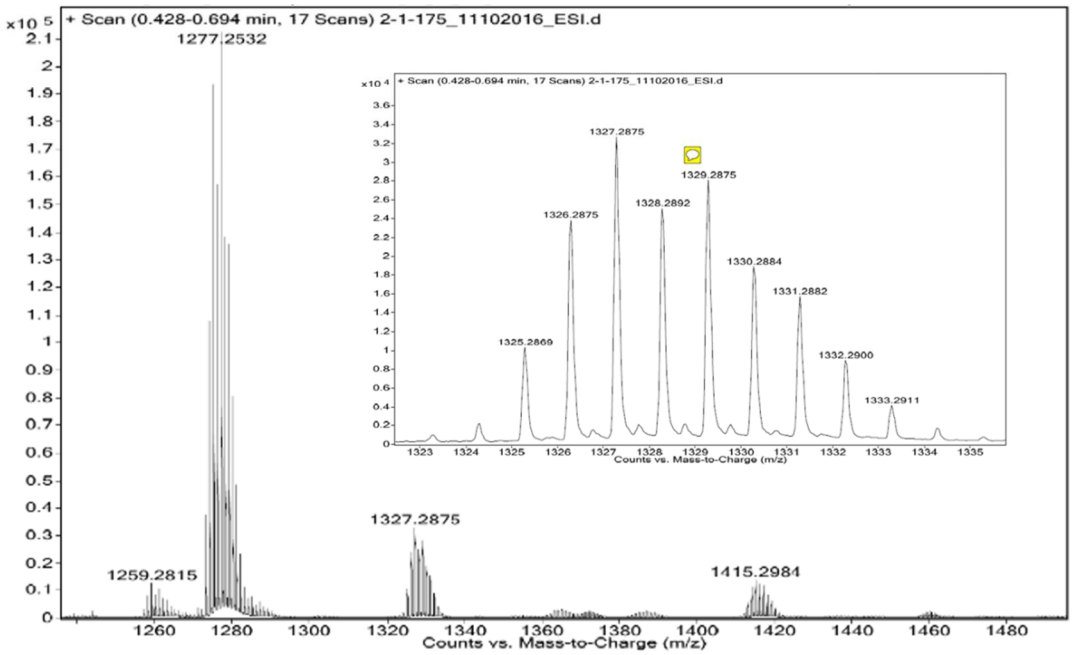

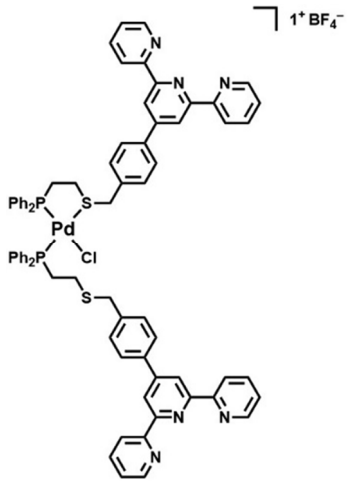
1+ BF4−
N
N
N
Ph2P
S
Pd
Ph2P
Cl
S
N
N
N

2-Pd-Open

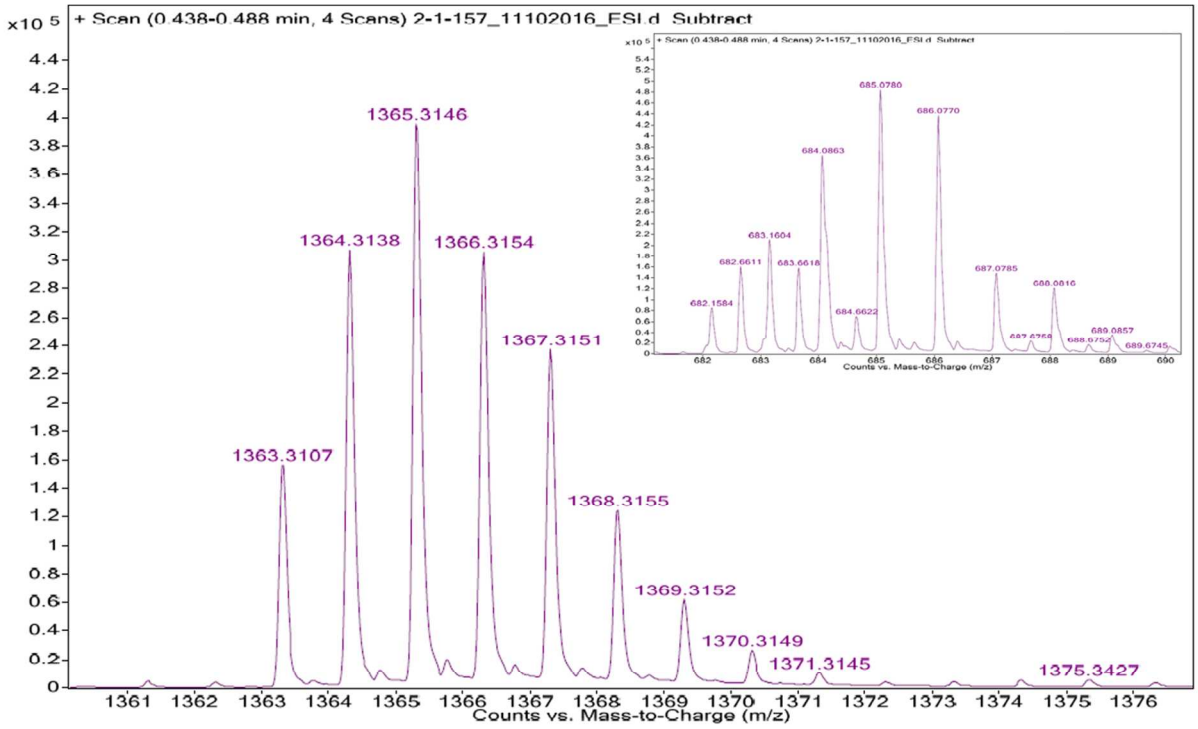
x10 5
+ Scan (0.438-0.488 min, 4 Scans) 2-1-157_11102016_ESI.d Subtract
1365.3146
1364.3138
1366.3154
1367.3151
1363.3107
1368.3155
1369.3152
1370.3149
1371.3145
1375.3427
Counts vs. Mass-to-Charge (m/z)

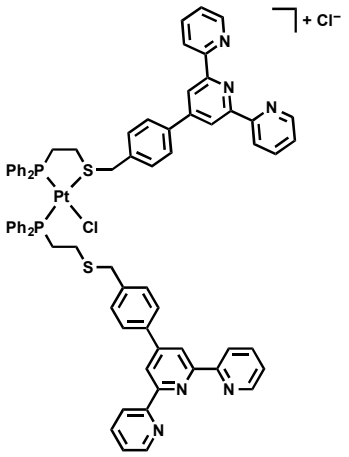
+ Cl⁻
N
N
N
Ph2P
S
Pt
Ph2P
Cl
S
N
N
N

2-Pt-Open

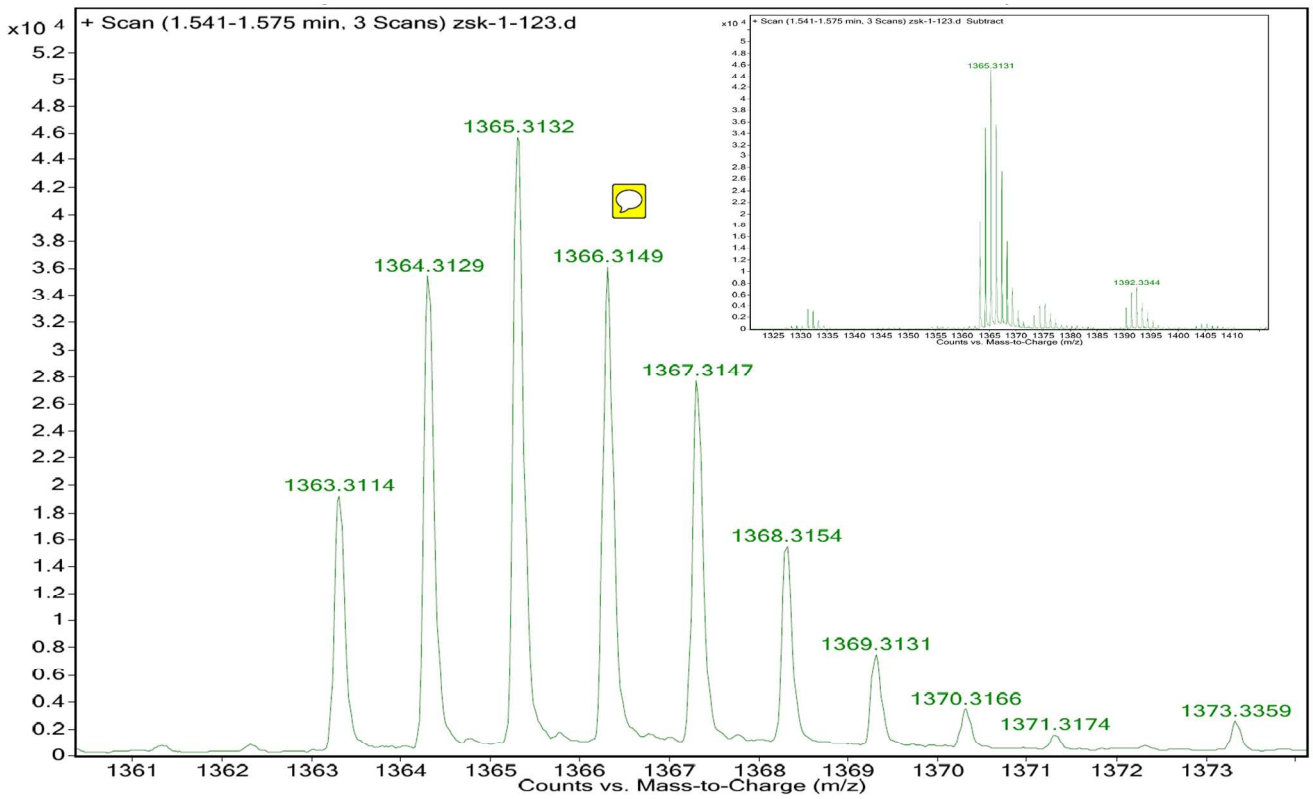
+ Scan (1.541-1.575 min, 3 Scans) zsk-1-123.d
x10 4
1365.3132
1364.3129
1366.3149
1367.3147
1363.3114
1368.3154
1369.3131
1370.3166
1371.3174
1373.3359
Counts vs. Mass-to-Charge (m/z)
+ Scan (1.541-1.575 min, 3 Scans) zsk-1-123.d Subtract
1365.3131
1392.3344
Counts vs. Mass-to-Charge (m/z)

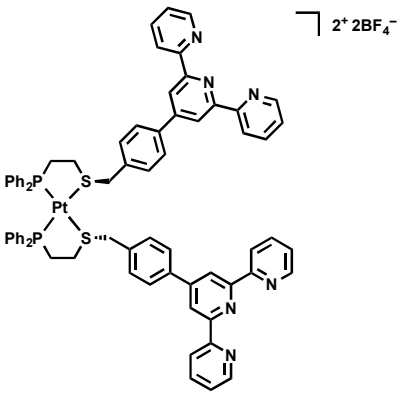
2+ 2BF4−
Ph2P
Pt
S
N

2-Pt-Closed

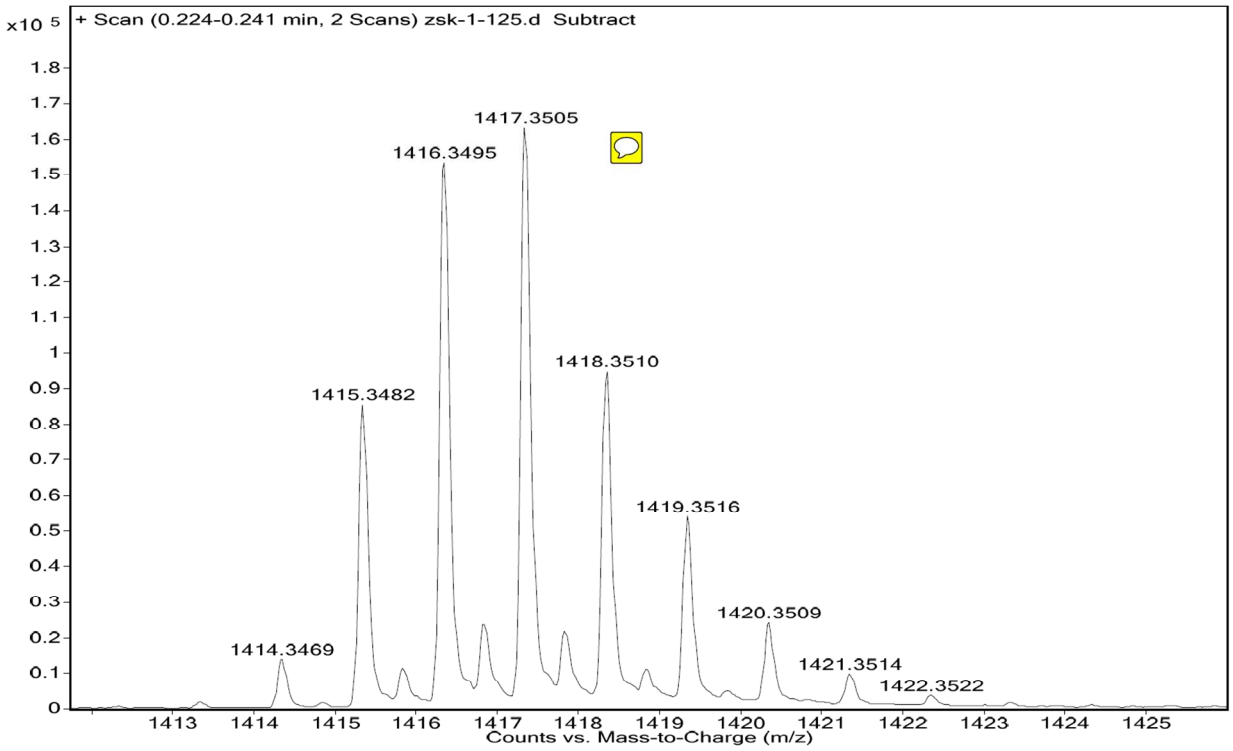
x10 5
+ Scan (0.224-0.241 min, 2 Scans) zsk-1-125.d Subtract
1417.3505
1416.3495
1418.3510
1415.3482
1419.3516
1420.3509
1414.3469
1421.3514
1422.3522
Counts vs. Mass-to-Charge (m/z)

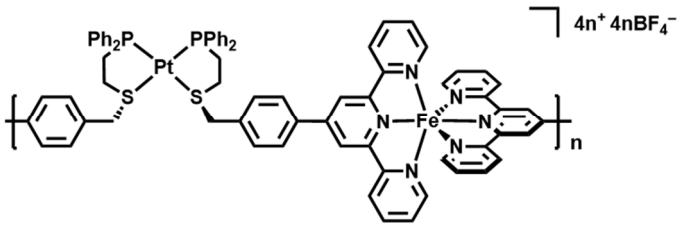

3-Pt-Closed

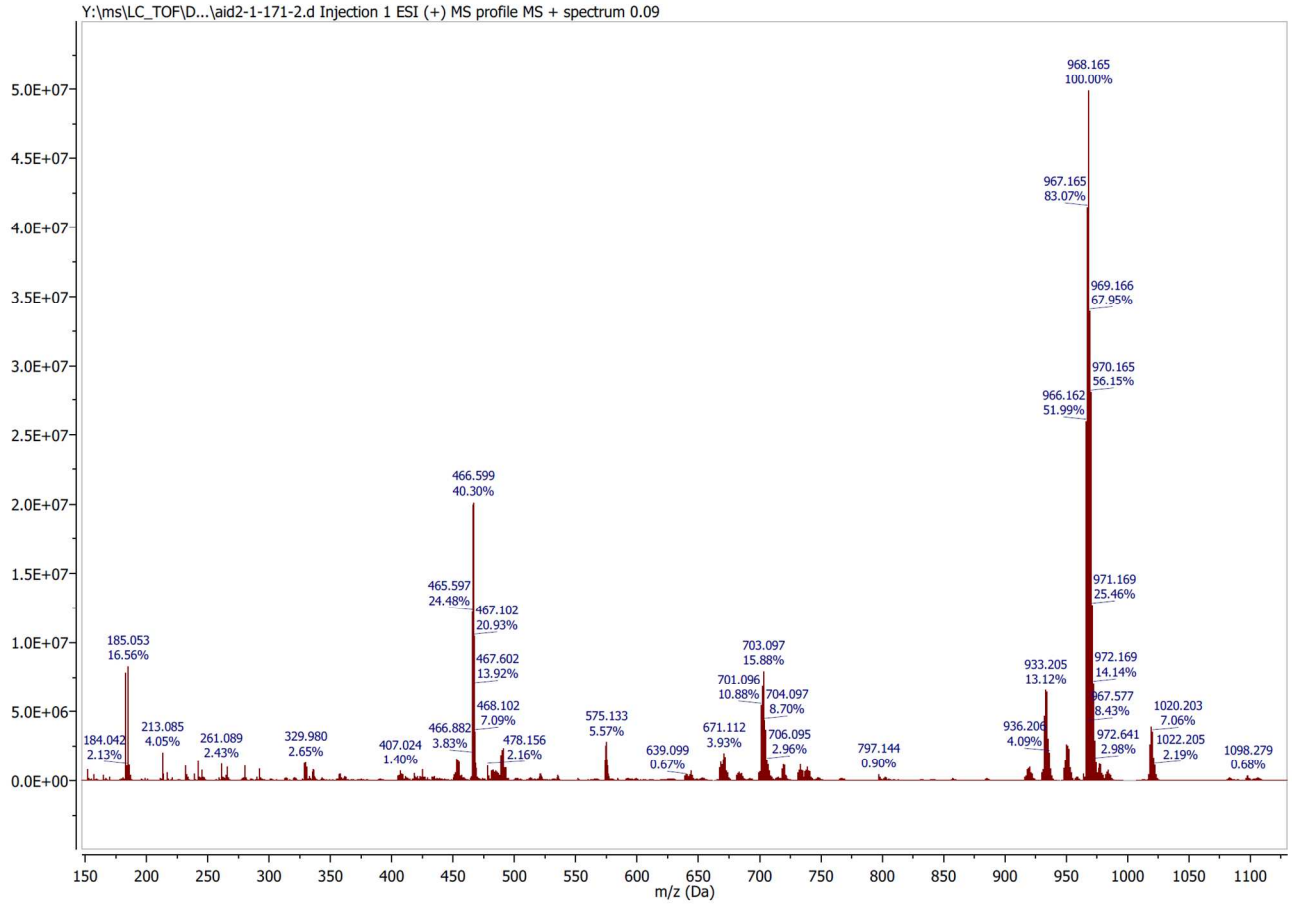

(fragments into multiple species)

References

(1) Ranaud, E.; Russell, R. B.; Fortier, S.; Brown, S. J.; Baird, M. C. Synthesis of a new family of water-soluble tertiary phosphine ligands and of their rhodium(I) complexes; olefin hydrogenation in aqueous and biphasic media. *J. Organomet. Chem.* **1991**, *419,* 403-415.
(2) Zhou, G.; Harruna, I. I. Synthesis and Characterization of Bis(2,2‘:6‘,2‘ ‘-terpyridine)ruthenium(II)-Connected Diblock Polymers via RAFT Polymerization. *Macromolecules* **2005**, *38,* 4114-4123.
(3) Dobrawa, R.; Ballester, P.; Saha-Möller, C. R.; Würthner, F. Thermodynamics of 2,2′:6′,2″-Terpyridine-Metal Ion Complexation. In *Metal-Containing and Metallosupramolecular Polymers and Materials*, American Chemical Society: 2006; Vol. 928, pp 43-62.
(4) Ernzerhof, M.; Scuseria, G. E. Assessment of the Perdew-Burke-Ernzerhof exchange-correlation functional. *J. Chem. Phys.* **1999**, *110,* 5029-5036.